Journal of Medicinal Chemistry

Article

pubs.acs.org/jmc

Identification of Glycogen Synthase Kinase-3 Inhibitors with a Selective Sting for Glycogen Synthase Kinase-3α

Fabio Lo Monte,*[,†] Thomas Kramer,[†] Jiamin Gu,[†] Upendra Rao Anumala,[†] Luciana Marinelli,[‡] Valeria La Pietra,[‡] Ettore Novellino,[‡] Bénédicte Franco,[§] David Demedts,[§] Fred Van Leuven,[§] Ana Fuertes,[∥] Juan Manuel Dominguez,[∥] Batya Plotkin,[⊥] Hagit Eldar-Finkelman,[⊥] and Boris Schmidt*[,†]

[†]Clemens Schöpf—Institute of Organic Chemistry and Biochemistry, Technische Universität Darmstadt, 64287 Darmstadt, Germany

[‡]Dipartimento di Chimica Farmaceutica e Tossicologica, Università di Napoli "Federico II", 80131 Napoli, Italy

[§]Experimental Genetics Group, Department of Human Genetics, Katholieke Universiteit Leuven, 3000 Leuven, Belgium

[∥]Noscira SA, Drug Discovery, Tres Cantos 28760-Madrid, Spain

[⊥]Department of Human Molecular Genetics and Biochemistry, Sackler School of Medicine, Tel Aviv University, 69978 Tel Aviv, Israel

Supporting Information

ABSTRACT: The glycogen synthase kinase-3 (GSK-3) has been linked to the pathogenesis of colorectal cancer, diabetes, cardiovascular disease, acute myeloid leukemia (AML), and Alzheimer's disease (AD). The debate on the respective contributions of GSK-3α and GSK-3β to AD pathology and AML is ongoing. Thus, the identification of potent GSK-3α-selective inhibitors, endowed with favorable pharmacokinetic properties, may elucidate the effect of GSK-3α inhibition in AD and AML models. The analysis of all available crystallized GSK-3 structures provided a simplified scheme of the relevant hot spots responsible for ligand binding and potency. This resulted in the identification of novel scorpion shaped GSK-3 inhibitors. It is noteworthy, compounds **14d** and **15b** showed the highest GSK-3α selectivity reported so far. In addition, compound **14d** did not display significant inhibition of 48 out of 50 kinases in the test panel. The GSK-3 inhibitors were further profiled for efficacy and toxicity in the wild-type (wt) zebrafish embryo assay.

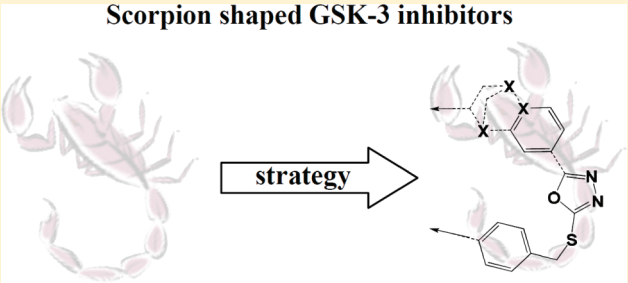

INTRODUCTION

Alzheimer's disease (AD), first described by Alois Alzheimer in 1906, is the most common dementia at old age. AD is characterized by the presence of two abnormal protein deposits: amyloid plaques composed of extracellular deposits of β-amyloid (Aβ) peptides and neurofibrillary tangles (NFTs) are formed by the accumulation of insoluble and hyperphosphorylated tau.[1−3] The 40−42 amino acid β-amyloid peptide is the major component of the amyloid deposits. It is produced from a larger protein, the amyloid precursor protein (APP), by proteolytic cleavage.[4] Tau is a soluble microtubule-binding protein which stabilizes the microtubules in axons.[2] Hyperphosphorylation of tau protein causes destabilization of microtubules and subsequent dissociation of tau, which in turn aggregates to form NFTs.[5] GSK-3 was identified ∼30 years ago and is a serine/threonine protein kinase that participates in a plethora of cellular processes, e.g., cell proliferation, microtubule dynamics, and gene transcription.[6−8] Several studies have linked glycogen synthase kinase-3 (GSK-3) to the primary abnormalities associated with AD, particularly the phosphorylation of tau.[4,9] Two closely related isoforms GSK-3α and GSK-3β are present in mammals.[10] They share 97% sequence similarity within their catalytic kinase domains.[7] GSK-3β has been proposed as the major kinase of tau phosphorylation, suggesting it as a potential, yet risky target for the therapy of AD.[1,5] Dysregulation of GSK-3β has been associated with diseases such as diabetes, Down's syndrome, bipolar disorder, colorectal cancer, and AD.[11] The inhibition of GSK-3α was suggested for the treatment of AD and other CNS diseases.[12−14] Furthermore, GSK-3α inhibition was proposed to modulate β-adrenergic signaling.[15] Recently, it was suggested that GSK-3α is involved in acute myeloid leukemia (AML), supporting a potential role for GSK-3α directed therapy.[16] Yet, the distinct contributions of both GSK-3 isoforms are still unknown. Appropriately, a number of pan-GSK-3α/β inhibitors have been disclosed because of the structure determination of GSK-3β.[17] Lithium chloride is the most thoroughly investigated GSK-3 inhibitor in AD animal models; it results in decreased tau hyperphosphorylation and decreased Aβ levels.[6] However, it is limited by a small therapeutic window. GSK-3 inhibitors were identified from remarkably different classes: organometallic compounds, paullones, indirubins, maleimides, thiadiazolidinones, L803-mts, ureas, and other small organic molecules.[4,10,18−24]

Received: March 5, 2012
Published: April 25, 2012

 © 2012 American Chemical Society

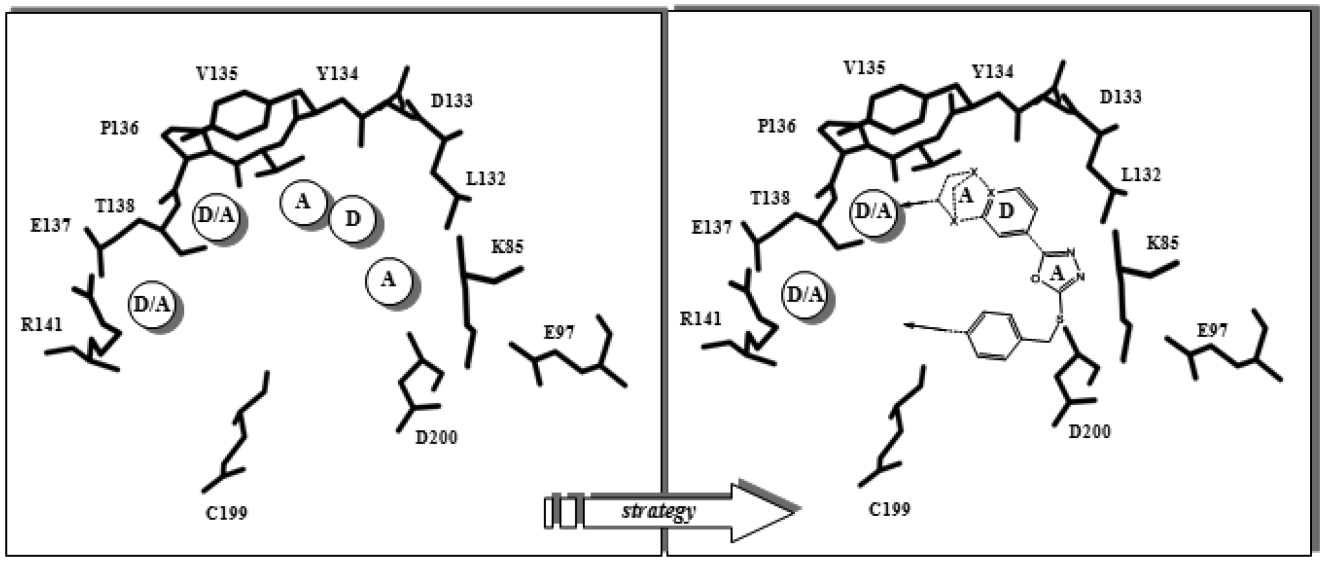

Figure 1. Synthesis strategy based on hot spot analysis of GSK-3 inhibition. The denoted acceptor (A) and donor (D) domains outline the necessary atoms respectively functional groups in the designated areas (left/right). The scaffold **I** used for the synthesis is marked on the right. X stands for heteroatoms.

Scheme 1[a]

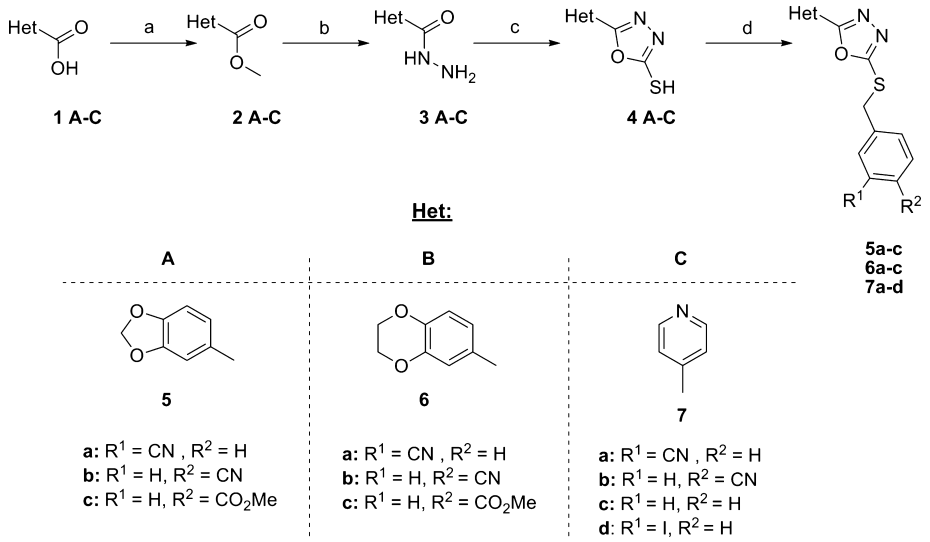

[a]Reagents and conditions: (a) MeOH, $SOCl_2$, 0−50 °C, 83−89%; (b) $NH_2NH_2{\cdot}H_2O$, EtOH, reflux, 67−75%; (c) CS_2, Et_3N, EtOH, reflux, 79−89%; (d) benzyl halides, 1N NaOH, DMF, rt, 41−84%.

All GSK-3 inhibitors, except for the thiadiazolidinones and L803-mts, are ATP competitive inhibitors and all of them inhibit the two isoforms, GSK-3α and GSK-3β, with similar potency.[6] The design of selective ligands remains a challenge despite several crystallized GSK-3 inhibitor complexes and substantial differences revealed by GSK-3α/GSK-3β sequence comparison as the major part of the ligand binding site is conserved.[17] Here we report the synthesis and optimization of novel GSK-3 inhibitors, along with their α/β selectivity and the evaluation of their in vivo efficacy in zebrafish embryos, which is an established model system for the validation of GSK-3 inhibitors. The oxadiazole moiety (scaffold **I**; Figure 1) was chosen as lead structure as it provided, if appropriately decorated, high inhibition of GSK-3β.[5,25,26]

The optimization process took advantage of the available cocrystallized GSK-3β inhibitor complexes and the analysis of the relevant hot spots (Figure 1). Most GSK-3 inhibitors occupy three or at most four acceptor/donor domains in the active site. Our main intention was the engagement with as many as possible acceptor/donor areas as depicted in Figure 1. Initially, we investigated the enlargement of **I** to reach R141. Subsequently, different substituents on the heterocyclic scaffold were explored in order to enhance the interaction with the enzyme backbone and to improve solubility at the same time. Most of the resulting compounds were tested for the selective inhibition of GSK-3α/β.

■ CHEMISTRY

The esterification of the carboxylic acids **1A−C** afforded the compounds **2A−C**,[27,28] which were converted to the hydrazides **3A−C**.[28,29] Reaction of the hydrazides **3A−C** with carbon disulfide (CS_2) resulted in the oxadiazoles **4A−C**.[30,31] The heterocyclic derivatives **5a−c**, **6a−c**, and **7a−c**[32] were prepared by benzylation of the mercaptanes **4A−C** (Scheme 1).[26]

Scheme 2[a]

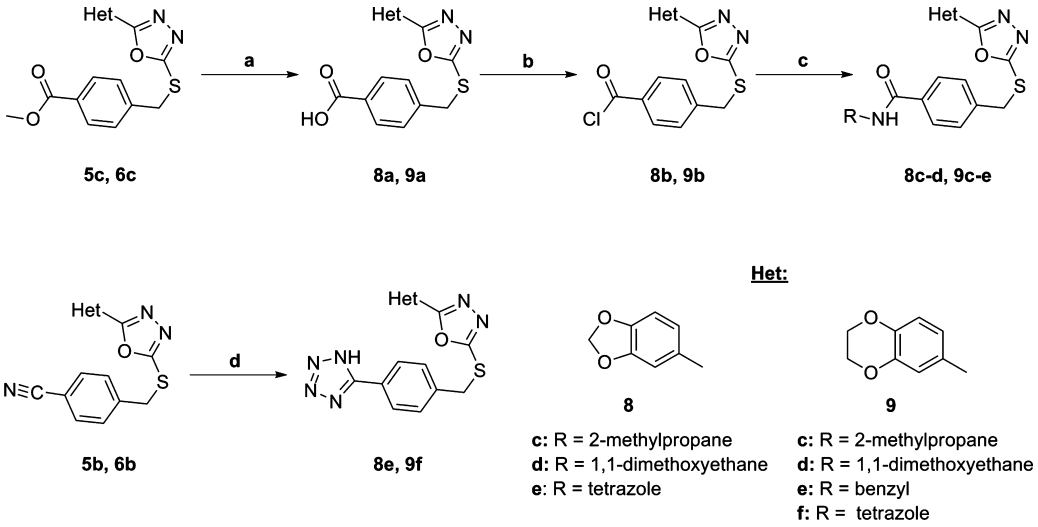

[a]Reagents and conditions: (a) 1N LiOH, THF, 60 °C, 83−91%; (b) $SOCl_2$, toluene, reflux; (c) amine, K_2CO_3, acetone, 0 °C to rt, 79−92%; (d) NaN_3, NH_4Cl, DMF, 100 °C, 67−79%.

Scheme 3[a]

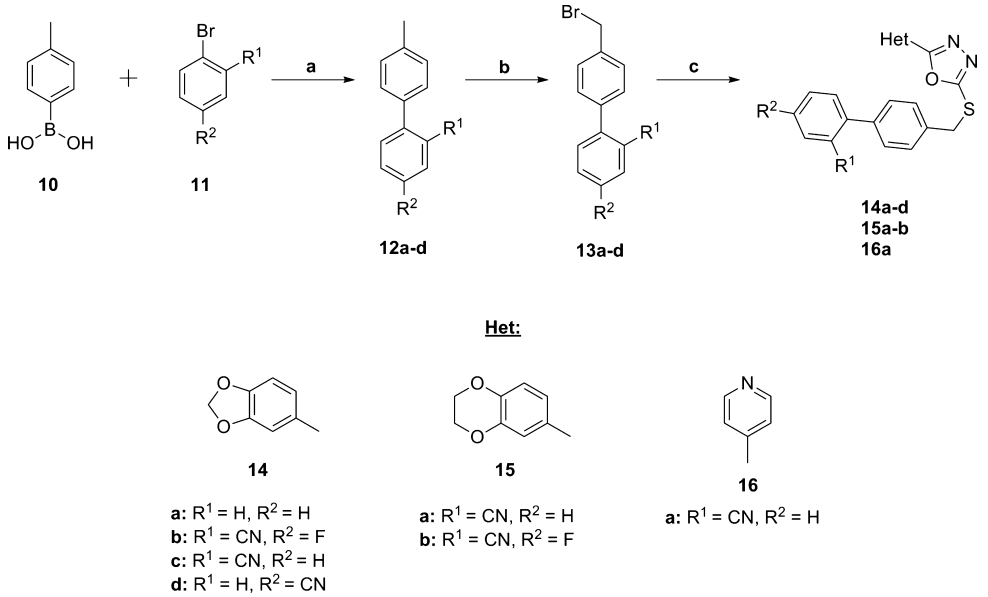

[a]Reagents and conditions: (a) aryl bromide, toluene, EtOH, $Pd(PPh_3)_4$, 2-tolylboronic acid, 2N Na_2CO_3 (aq), 80 °C; (b) NBS, AIBN, CCl_4, reflux; (c) **4**(**A**−**C**), 1N NaOH, DMF, rt, 53−75%.

Compound **7d** is commercially available. The esters **5c** and **6c** were converted to the carboxylic acids **8a** and **9a**, followed by treatment with thionyl chloride ($SOCl_2$) to form the acyl chlorides **8b** and **9b**.[33,34] Coupling of the acyl chlorides with primary amines gave the amides **8c**−**d** and **9c**−**e**.[34] The tetrazoles **8e** and **9f** were prepared from the nitriles **5b** and **6b** using sodium azide under microwave irradiation (Scheme 2).[35]

The biphenylic derivatives **13a**−**d** were prepared in two steps from the commercially available *p*-tolylboronic acid and substituted bromobenzenes. The 4′-(bromomethyl)biphenyl-2-carbonitrile is commercially available. The biphenylmethyl halides were coupled to the mercaptothiadiazoles **4A**−**C** to obtain the thioethers **14a**−**d**, **15a**−**b**, and **16a** (Scheme 3).[26] 3,4-Dihydroxybenzoic acid **17** was esterified to the methyl ester **18**, followed by cyclization with (±)-glycidyl tosylate or epibromohydrin to afford compound **19a**[36] as a mixture of enantiomers.[37−39] The hydrazide **21a** was prepared by methylation of **19a**, followed by the addition of hydrazine.[40] The reaction of the hydrazide **21a** with CS_2 gave the oxadiazole **22a**, which was coupled to 4′-(bromomethyl)biphenyl-2-carbonitrile to afford the thioether **23a**. The methyl ether in **23a** was cleaved by boron tribromide (BBr_3) to result in the alcohol **24a** (Scheme 4).[40] The compounds **23b**−**c** and **24a**−**b** were prepared under similar conditions; see Scheme 4. (*S*)-(+)-Glycidyl tosylate was used to obtain the *R*-enantiomer of compound **19b**.[37] The *S*-enantiomer of compound **19** was synthesized using (*R*)-(−)-glycidyl tosylate.[37] Mesylation of the alcohol **24b** and subsequent displacement of the mesylate by an amine afforded the acetal **26** (Scheme 4).[40]

Scheme 4[a]

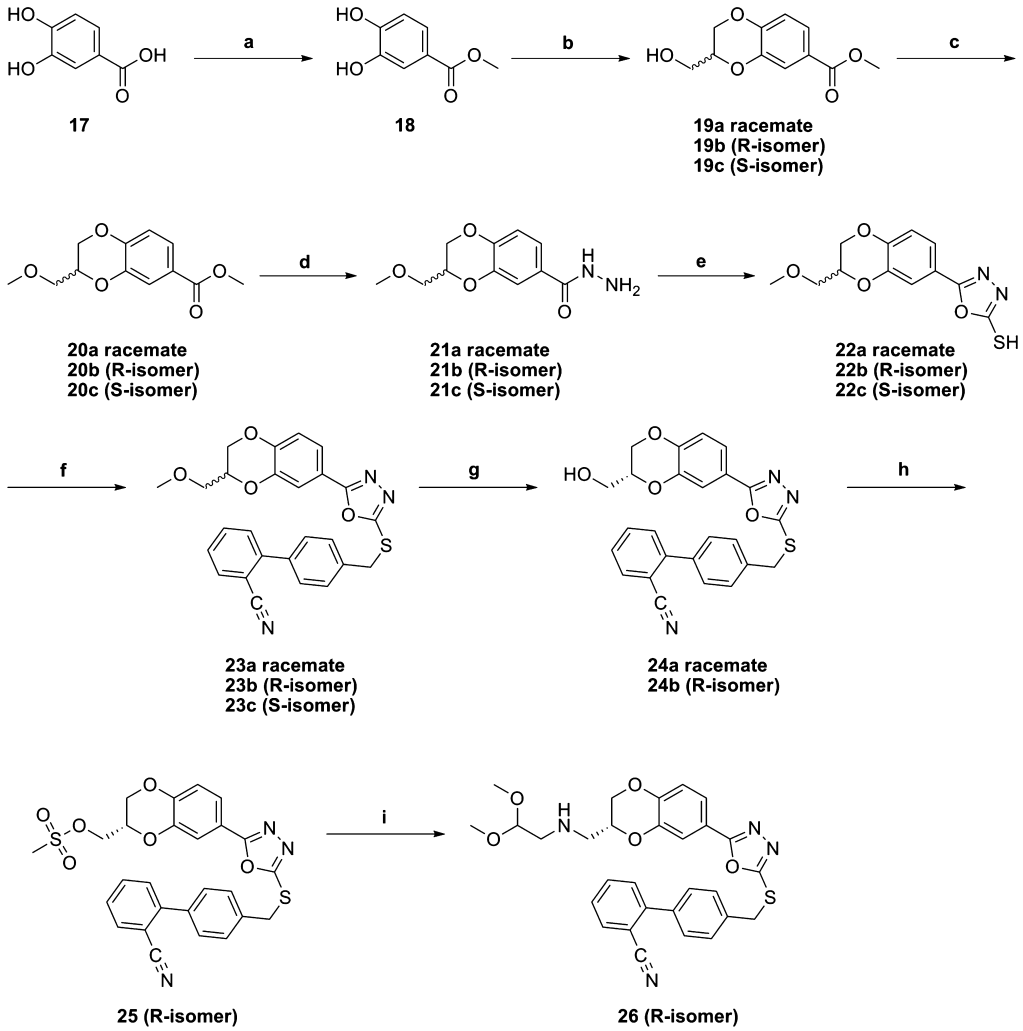

[a]Reagents and conditions: (a) $SOCl_2$, MeOH, 0−50 °C, 97%; (b) (*R*/*S*)-(±)-glycidyl tosylate or epibromohydrin, (*S*)-(+)-glycidyl tosylate or (*R*)-(−)-glycidyl tosylate, K_2CO_3, acetone or DMF, rt or 60 °C, 93−95%; (c) NaH, CH_3I, THF, 0 °C to rt, 68−71%; (d) $NH_2NH_2{\cdot}H_2O$, EtOH, reflux, 78−87%; (e) CS_2, Et_3N, EtOH, reflux, 81−91%; (f) biphenyl halide, 1N NaOH, DMF, rt, 84−88%; (g) BBr_3, DCM, −78 °C to rt; 73−79%; (h) CH_3SO_2Cl, Et_3N, DCM, 0 °C to rt, 98%; (i) amine, THF, Et_3N, 0 °C to reflux, 83%.

RESULTS AND DISCUSSION

Molecular Modeling. Compound **15a**, one of the most active inhibitors of the series, was docked, through Glide software, into the GSK-3β active site (PDB code: 3F88) with the aim to assess the ligand−protein interactions and to rationalize the SARs.[26] The docking experiments suggest that the oxadiazole ring positions itself in between the V70 and C199 side chains with one of the two nitrogens establishing an H-bond with the K85 side chain (Figure 2). The biphenyl branch forms a T-shaped interaction with P67 and hydrophobic contacts with the Q185 and Y140 carbons.[41] Furthermore, as shown in Figure 2, the CN substituent forms an H-bond with the T138 hydroxyl group. The latter interaction seems to improve the activity of our ligands, in fact, for example, **14c** is more active against GSK-3β than its analogue **14a**, which lacks the cyano group, and its analogue **14d**, equipped with the cyano group at the R2 site. As regards the **15a** binding mode, the dihydrobenzodioxine moiety establishes several hydrophobic interactions with L132, I62, A83, V110, and L188.

Moreover, one of the two oxygens of the dihydrodioxine ring forms an H-bond with the V135 NH in the hinge region, while

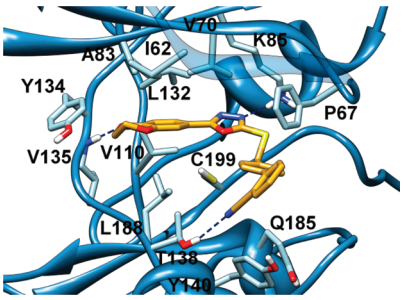

Figure 2. Molecular docking of compound **15a** into the X-ray structure of GSK-3β (PDB code: 3F88). This figure was prepared with Glide software.

the rest of the ring establishes hydrophobic contacts with the Y134. The latter interaction seems to be lost by **14c**, featuring the smaller benzodioxolane ring, while **16a**, a pyridine containing compound, forms a weaker H-bond with the same residue due to the position and the distance of the nitrogen atom of the pyridine ring from the NH of V135. The substitutions on the dihydrobenzodioxine moiety of **23** and **24**,

respectively, do not provide any further interaction with the enzyme, as the groups point out into the solvent. The same holds true for **26**, where the bulky substituent on the dihydrobenzodioxine ring may negatively affect the horseshoe shape (scorpion shape). The proposed binding mode also clarifies the undesirable effect of the substitution of the fluorine atom at the R2 site of the biphenyl branch in **15b**, which is 37-fold less potent for GSK-3β in comparison to **15a**. In fact, the electron-withdrawing atom weakens the H-bond between the cyano substituent and the T138 hydroxyl group; moreover, it comes in proximity of the negative ring density of Y140, providing repulsive edgewise interaction. The good selectivity toward GSK-3α versus GSK-3β which was observed for several compounds and especially for compound **15b**, is far to be trivial to explain. The superposition of the GSK-3β crystallographic structure (PDB code: 3F88) with a homology model built with Prime software (Schrodinger) shows that the differences between the two isoforms are all located out of the binding site and especially in the loop at C-terminus fragment (see the Supporting Information). Thus, it is conceivable that the selectivity of our compounds may be due to subtle enzyme differences, which may affect the ligand entrance/exit processes. This process may include an antechamber site, a step known to play a pivotal role in the inhibitor/enzyme recognition process.[42,43] By analyzing the enzyme surface and the residue mutations, the antechamber site in the GSK-3α or GSK-3β could be represented by the loop at C-terminus fragment as highlighted in Figure S1 in the Supporting Information. Obviously, the latter is a pure speculative hypothesis that has to be confirmed by more advanced theoretical work, mutational analysis, and additional experiments.

Biological Assays and Structure−Activity Relationship (SAR) Studies. The synthesized compounds were tested for their inhibitory activity against GSK-3β in an in house in vitro assay and further profiled in a commercial system based on the Z'-LYTE technology, available from Invitrogen Life Technologies (Carlsbad, CA, USA), using human recombinant GSK-3α or GSK-3β as the enzyme source. Most compounds displayed significant inhibitory activity against GSK-3β at 10 μM, and several compounds exerted more than 50% inhibitory activity against GSK-3β at the initial concentration (10 μM). The potent compounds were selected for IC_{50} determination. We observed differences in the IC_{50} determination between the in-house and the commercial assay and decided to use the results of the commercial system for comparison.

The structure−activity analysis suggested interactions with the GSK-3 backbone, Y134/D133, and the polar binding pocket, K85/E97/D200, to be essential for potent inhibition. These interactions require an acceptor−donor−acceptor motif on the inhibitor. We generated a simplified illustration in which we denoted acceptor (A) and donor (D) domains and drafted scaffold **I** as lead structure (Figure 1). We examined the effect of three heterocycles **5**−**7** as potential hinge binders and different substituents on the *S*-benzyl group (Scheme 1). The oxadiazole derivatives of the heterocycles **5** and **6** provided several GSK-3 inhibitors with an IC_{50} below 100 nM (Table 1) and confirmed previously reported activity.[26] The pyridines **7a**−**c** displayed decreased activity in comparison to the heterocycles **5** and **6**; this may be due to the position of the pyridine moiety in the ATP binding pocket. Thus, they were not pursued further. The compounds **5a** and **6a** indicated that an electron-withdrawing group is required at the 3-position. We introduced the cyano and ester group at the 4-position in order to reach out to R141 and the correlated acceptor/donor domain and thus to engage the ATP binding pocket in its entirety. Our data indicated that the electron-withdrawing group at the 3-position was also tolerated at the 4-position. The oxadiazoles **5b** and **6b**−**c** showed comparable activity to the 3-substituted derivatives and indicated space in the ATP binding pocket. On the basis of these results, we further examined the para-position of our lead structure. The carboxylic acids **8a** and **9a** resulted in a 4-fold less inhibitory activity against GSK-3β at 10 μM concentration compared to their esters **5c** and **6c** (Scheme 2). In the case of **5c**, the percentage of GSK-3β activity increased from 17% of up to 81% (Table 2). In addition, compound **8e**, bearing a hydrophilic tetrazole at the 4-position (IC_{50} value of 107 nM for GSK-3α and 172 nM for GSK-3β), showed decreased inhibitory activity compared to the ester **6c** (Scheme 2). Conversion of the carboxylic acids to the amides **8c**−**d** and **9c**−**e** resulted in an increased activity. Especially, compound **8c** showed good inhibitory property against GSK-3β with a remaining kinase activity of 9% at 10 μM (Table 2). These results and the molecular modeling suggested that compounds containing polar groups at the 4-position were less active than compounds containing hydrophobic groups. Hence, we tried to elongate our compounds with a phenyl ring at the 4-position. Compounds bearing a phenyl group in the para-position showed very good inhibitory activity. The docking analysis of the biphenylic derivatives suggested several hydrophobic contacts, which may be responsible for the enhanced potency. Especially, compound **15a** with an IC_{50} value of <5 nM for GSK-3α and GSK-3β was found to be a potent inhibitor of GSK-3 (Table 3). Slightly decreased activity was observed for compound **14a** with an IC_{50} value of 9 nM for GSK-3α and 176 nM for GSK-3β. We observed an IC_{50} of 2 nM for GSK-3α and 22 nM for GSK-3β for structure **14b**, whereas **14c**, which lacks the fluorine substituent, resulted in slightly decreased IC_{50} values in comparison to **14b**.

The selectivity for the GSK-3α isoform was higher when the substituents were absent in the series **14a**−**c**. The absence of selectivity for GSK-3α in **15a** in comparison with **14c** may be explained by the interaction with Y134 (see Molecular Modeling), which seems to be lost in **14c**. Remarkably, compound **14d** displayed up to 52-fold selectivity in the inhibition of GSK-3α versus GSK-3β. This selectivity was even enhanced with compound **15b**, which is characterized by an IC_{50} of 2 nM for GSK-3α and 185 nM for GSK-3β. Thus, only the interplay respectively of a combination of different substituents was adequate to gain selectivity against one GSK-3 isoform. This observation will be helpful if a discrimination of one GSK-3 isoform is needed. In addition, the physiological functions and pathological roles of GSK-3α can be addressed in vitro and eventually in vivo with these tools. The biphenyl derivative **16a** from the pyridine series showed remarkably increased activity in comparison to the used reference **7d**, 20-fold for GSK-3α, and 19-fold for GSK-3β (Table 1). The effect of the second phenyl suggested an interaction with the glycine-rich loop, such an interaction was reported to have significant effects on binding potency and selectivity recently.[41] Furthermore, the SAR and molecular modeling suggested that an electron-withdrawing group in the ortho position of the second phenyl ring, such as the cyano-group, contributes to the inhibitory activity by interaction with the amino acid T138. We examined different linker systems on the dihydrobenzodioxine moiety with the aim to enhance the interaction with the backbone. Unfortunately, they do not provide any further

Table 1. Inhibitory Activity against GSK-3α and GSK-3β, IC_{50} (μM)

Compound	GSK-3α	GSK-3β	Compound	GSK-3α	GSK-3β
5a	0.015	0.065	**7a**	3.206	3.162
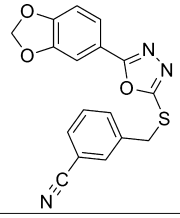			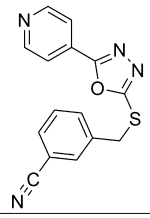		
5b	0.015	0.130	**7b**	7.379	10.0
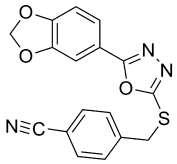			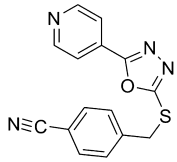		
6a	0.095	0.086	**7c**	2.244	1.318
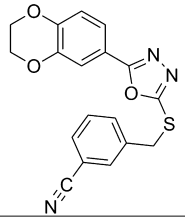			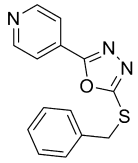		
6b	0.045	0.166	**7d**	0.390	0.790
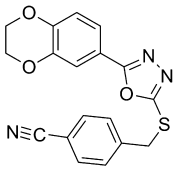			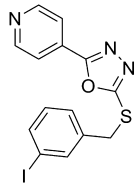		
6c	0.012	0.036	**8e**	0.107	0.172
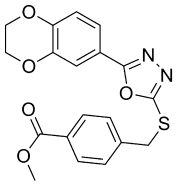			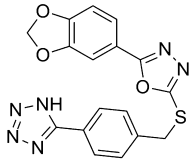		

interaction (see Molecular Modeling). The effect of the methoxy group on compound **23a** resulted in an IC_{50} value of 54 nM for GSK-3α and 233 nM for GSK-3β, respectively, 195 nM and 758 nM for compound **23b**. In the case of **23c**, good inhibitory activity was observed against both isoforms of GSK-3, especially for GSK-3α. These results suggest that the *R*-enantiomer **23b** is the distomer of this compound, whereas the *S*-enantiomer **23c** was found to be the eutomer. Despite our expectations that an amine may improve the activity, compound **26** showed markedly reduced potency.

The potent GSK-3 inhibitors **6c**, **14a–d**, **15a–b**, **16a**, and **23a–c** were selected for selectivity profiling and tested against four structurally related protein kinases (Cdk5/p35, CK1ε, AurKA, and PKCα).

Good selectivity was obtained for all compounds tested. Particularly, the biphenyl derivatives **14c**, **15a**, and **16a** showed more than 2000-fold selectivity against these kinases (Table 4). Compound **14d** was not just GSK-3α selective, it was even more selective over the other kinases than compound **15b**. The broader selectivity of compound **14d** was screened at a concentration of 1 μM against 50 human protein kinases (Figure 3); 48 out of the 50 kinases in this panel showed an activity higher than 80%, whereas GSK-3α displayed a residual activity of 5% only. The only kinase which was also significantly inhibited by this compound was GSK-3β with a remaining activity of 27.2%. Therefore, it can be concluded that, within the test panel, compound **14d** is a selective inhibitor of GSK-3α. A bioavailability profile of compound **14d** was evaluated,

Table 2. Inhibitory Activity against GSK-3β at 10 μM

Compound	GSK-3β activity in %	Compound	GSK-3β activity in %	Compound	GSK-3β activity in %
5c 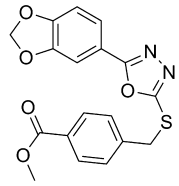	17	**8c** 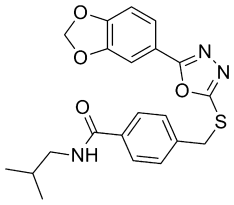	9	**9c** 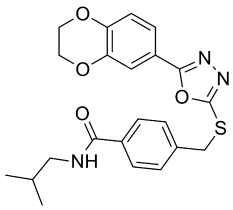	37
6c 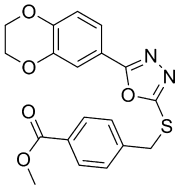	21	**8d** 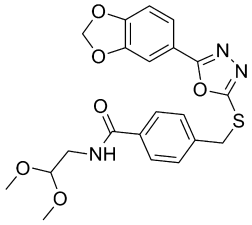	31	**9d** 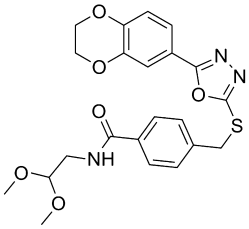	65
8a 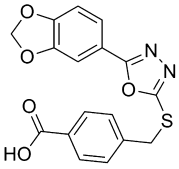	81	**9a** 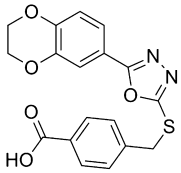	102	**9e** 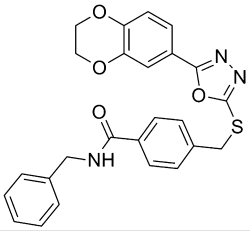	71

and the results are shown in the Supporting Information. **14d** possesses a log *D* value of 3.58 and moderate metabolic stability. Nevertheless, the poor aqueous solubility and permeability are adverse properties which limit the potential use of the compound.

The biphenyl derivatives **14c–d**, **15a–b**, and **16a** were further tested for their in vivo activity on wild-type zebrafish embryos. We exposed the embryos to these compounds at early stages of development. The embryos were collected and maintained in E2 medium at ~28 °C. The compounds were added 5 h post fertilization (hpf), and the phenotypes compared at 44–48 hpf. Compound **14c** causes the eyeless phenotype at 0.5 μM and a stunted and crooked tail at 1 μM. Similar phenotypes were obtained for compound **15a** at 2.5 μM and for compound **16a** at 20 μM (Figure 4). This correlates with the observation that Wnt signaling, and thus GSK-3β plays a crucial role in the development of metazoan and that known GSK-3 inhibitors like LiCl and the ruthenium complex (*R*)-**7** perturb the zebrafish development.[44,45] The zebrafish embryo assay provides evidence of exposure and cell penetration of the biphenyl derivatives, especially for compound **14c**. Interestingly, compounds **14d** and **15b** showed no effect on wild-type zebrafish embryos, suggesting that GSK-3α plays a minor role in the zebrafish Wnt signaling pathway. The lack of response in the zebrafish assay by compounds **14d** and **15b** may be explained by poor cell permeability. However, the structurally analogues compounds **14c** and **15a**, which are characterized by comparable solubility, did result in a GSK-3β-phenotype. Thus, the comparison of these compounds **14c**/**15a** and **14d**/**15b** does not support poor exposure and cell penetration as the dominant factors on the in vivo assay of the α-selective inhibitors. The inhibition of GSK-3α was proposed to regulate β-adrenergic signaling in mice, thus we monitored the heart development of the zebrafish embryo after administration of compound **14d** until day 5 (see the Supporting Information).[15,46] However, no effect was observed until the fifth day of development. All compounds displayed no lethality in our concentration range (<30 μM).

SH-SY5Y neuroblastoma cells stably transfected with Tau.P301L were incubated with increasing concentrations of compounds **14c** and **15a** (0, 30, and 100 μM) for 6 and 24 h. Cells were analyzed for total protein tau by Western blotting with antibody Tau5, directed against nonphosphorylated protein tau. In addition, the same samples were probed with a selection of phospho-specific antibodies that recognize typical GSK-3 dependent epitopes on protein tau. Moreover, the electrophoretic mobility of protein tau is a reliable index of the degree of phosphorylation of protein Tau.P301L: the lesser mobile isoforms carry the most phosphate groups (Figure 5).

Both compounds dose- and time-dependently decreased the phosphorylation of protein tau, expressed relatively to total tau, as demonstrated by the decreased immunoreaction with antibodies pS199, pT231, pS396, and pS404 in Western blotting (Figure 5). Moreover, the marked increase in electrophoretic mobility of the various phospho-isoforms of protein tau induced by treatment of the stably transfected SH-SY5Y cells corroborates their effectiveness in preventing phosphorylation on typical GSK-3 dependent epitopes. The comparison of the biphenyl derivatives indicated that compound **14c** is more effective in preventing phosphorylation than compound **15a**.

Table 3. Inhibitory Activity of the Biphenyls against GSK-3α and GSK-3β, IC_{50} (μM)

Compound	GSK-3α	GSK-3β	Compound	GSK-3α	GSK-3β
14a	0.009	0.176	**15b**	0.002	0.185
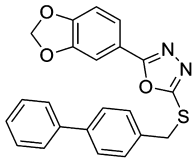			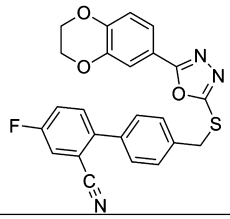		
14b	0.002	0.022	**16a**	0.019	0.041
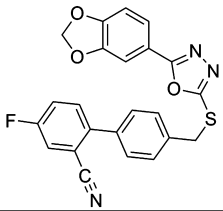			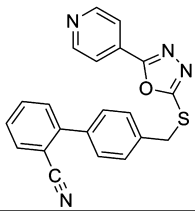		
14c	< 0.005	0.039	**23a**	0.054	0.233
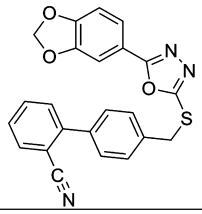			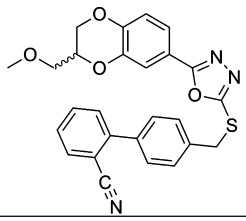		
14d	0.006	0.316	**23b**	0.195	0.758
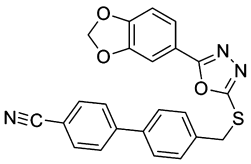			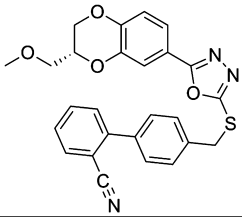		
15a	< 0.005	< 0.005	**23c**	0.015	0.129
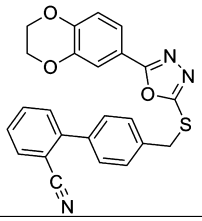			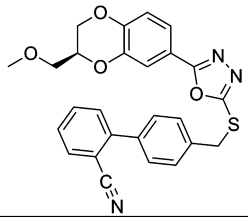		

This correlates with the observations made in the zebrafish embryo assay in which **14c** showed the best results.

■ CONCLUSION

On the basis of a simplified scheme of known and important interactions of GSK-3 inhibitors with the ATP binding pocket, we generated hypotheses for improved interaction of with this site. These hypotheses were challenged by three series of structurally closely related inhibitors which are all based on a central oxadiazole moiety. An appropriate decoration resulted in a more extended occupation of the ATP binding site. The most potent inhibitors displayed IC_{50} values in the low nanomolar range and good kinase selectivity versus four closely related kinases. Several inhibitors showed reported phenotypes in the zebrafish embryo assay without lethality at 30 μM. In addition, two inhibitors decreased the phosphorylation of tau protein in SH-SY5Y cells. The docking analysis of the potent inhibitors suggested an interaction with the glycine-rich loop, which was reported to have significant effects on the binding potency and selectivity by Li Feng et al.[41] To our knowledge, the selective inhibition of GSK-3α versus GSK-3β by the compounds **14d** and **15b** is the highest reported so far. In addition, compound **14d** did not show any strong inhibition for 48 out of 50 kinases. The contribution of GSK-3α and GSK-3β to the pathology of Alzheimer's disease is still subject of an ongoing debate.[47,48] Thus, these compounds may be useful tools and starting points for the synthesis of GSK-3α selective inhibitors with enhanced pharmacokinetic properties.

Table 4. Kinase Selectivity of Several Derivatives

	IC_{50} (μM)					
compd	GSK-3α	GSK-3β	Cdk5/p35	CK1ε	AurKA	PKCα
6c	0.012	0.036	>100	>100	>100	>100
14a	0.009	0.176	>100	>100	>100	>100
14b	0.003	0.022	>100	20	30	>100
14c	<0.005	0.039	>100	>100	>100	>100
14d	0.006	0.316	>100	60	30	>100
15a	<0.005	<0.005	>100	>100	>100	>100
15b	0.002	0.185	>100	>100	5	>100
16a	0.019	0.041	>100	>100	>100	>100
23a	0.054	0.233	>100	>100	30	>100
23b	0.195	0.758	>100	>100	>100	>100
23c	0.015	0.129	>100	>100	>100	>100

■ EXPERIMENTAL SECTION

General Information. All reactions using anhydrous conditions were carried out under argon atmosphere with dry solvents unless otherwise noted. All commercial chemicals were used without further purification. The ^{1}H NMR spectra were recorded on a Bruker AC 300 spectrometer at 300 MHz and Bruker AC 500 spectrometer at 500 MHz. The ^{13}C NMR spectra were recorded on a Bruker AC 300 spectrometer at 75 MHz and Bruker AC 500 spectrometer at 125 MHz. Chemical shifts are reported as ppm downfield from Me_4Si. Abbreviations used to explain the multiplicities: s = singlet, d = doublet, t = triplet, q = quartet, n = nonett, m = multiplet, br = broad. Coupling constants (J values) are given in hertz (Hz). Mass spectrometry was performed on a Bruker–Franzen Esquire LC mass spectrometer and a MAT 95 double focusing sector field MS. Microwave experiments were carried out using a Biotage Initiator microwave apparatus. All microwave experiments were carried out in sealed microwave process vials utilizing the standard absorbance level (300 W maximum power). High performance liquid chromatographies (HPLC) were carried out on an Agilent 1100 (column: reversed phase, Zorbax Eclipse XDB-C18, 4.6 mm × 150 mm; 254 nm). Solvent gradient = 90% A at 0 min, 30% A at 2 min, 10% A at 5 min; solvent A = 0.1% trifluoroacetic acid in water; solvent B = acetonitrile; flow rate 1.0 mL/min; temperature 35 °C. Flash column chromatography was carried out using Merck silica gel 60 (40–63 and 15–40 μm) and 60G (5–40 μm). Thin-layer chromatography (TLC) was carried out using aluminum sheets precoated with silica gel 60 F254 (0.2 mm; E. Merck). All compounds that were evaluated in biological assays had >95% purity using the HPLC method described above.

General Procedure A: Coupling of Aromatic Rings by a Suzuki Reaction (12a–d).[49] To a solution of the aryl bromide **11** (5 mmol) in 15 mL of toluene/EtOH (1/1) was added 0.17 g (0.14 mmol) of $Pd(PPh_3)_4$, and the mixture was stirred under argon atmosphere. Then 2 N aqueous Na_2CO_3 (7.5 mL) and 0.80 g (6 mmol) of 2-tolylboronic acid **10** were added. The mixture was refluxed at 80 °C for 1–2 days until reaction was completed (TLC). After cooling to room temperature, the product was diluted with water and extracted with EtOAc. The organic layers were dried with $MgSO_4$, filtered, and concentrated. Purification was performed by column chromatography using a mixture of cyclohexane/EtOAc.

General Procedure B: Bromination at the Benzylic Position (13a–d).[49] To a stirred solution of the appropriately substituted toluene in CCl_4 (10 mL per mmol) were added 0.95 equiv of NBS and AIBN (5 mg per mmol). The reaction mixture was refluxed at 80 °C for about 40 h and then cooled to room temperature. The product was diluted with water and extracted with EtOAc. The organic layers were dried with $MgSO_4$, filtered, and concentrated. Purification was performed by column chromatography using a mixture of cyclohexane/EtOAc.

Methyl Benzo[*d*][1,3]dioxole-5-carboxylate (2A). To a stirred solution of benzo[*d*][1,3]dioxole-5-carboxylic acid (1.66 g, 10 mmol) in MeOH (20 mL) was added $SOCl_2$ (1.45 mL, 20 mmol) dropwise over 1 h at 0 °C. The mixture solution was further stirred 12 h at 50 °C. The mixture was cooled to room temperature and diluted with water (25 mL). MeOH was evaporated and the pH adjusted to ~6 with aqueous $NaHCO_3$. The mixture was extracted three times

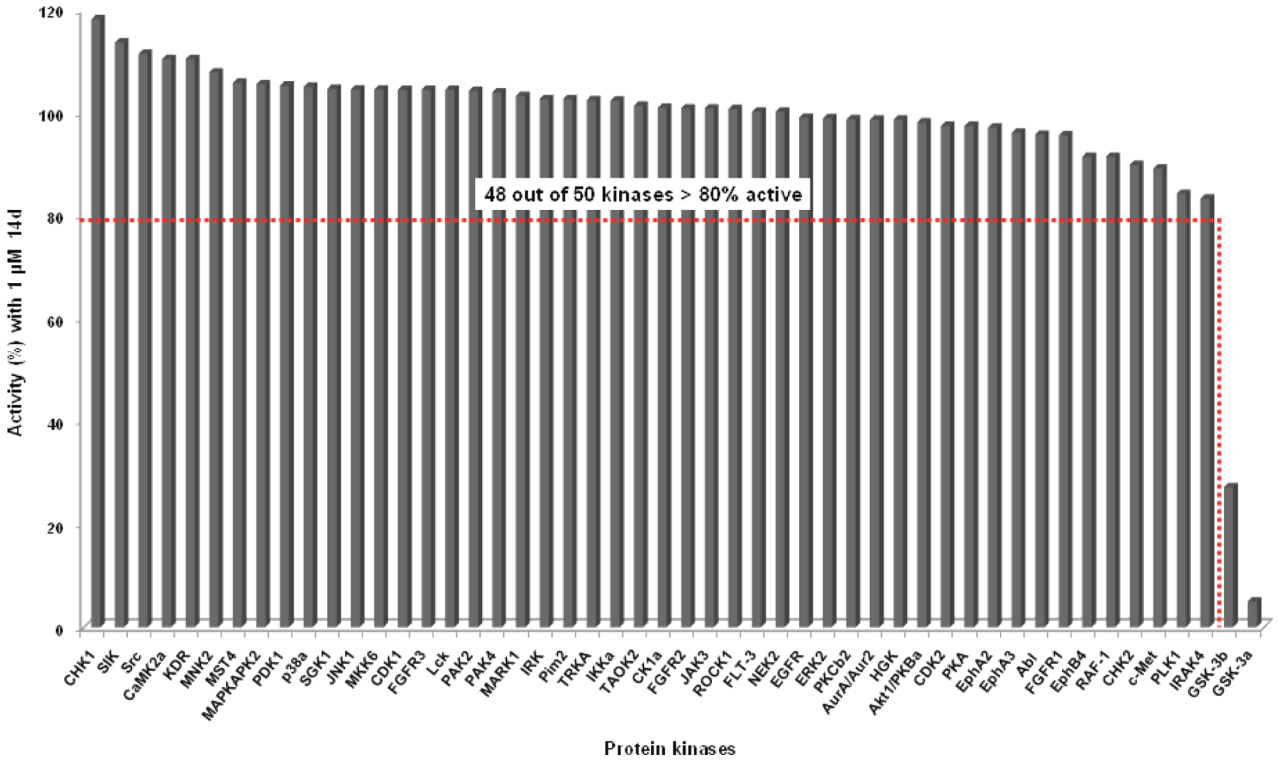

Figure 3. Screening of compound **14d** against a panel of human protein kinases. Each bar represents the activity of one individual protein kinase. Compound **14d** was tested at a concentration of 1 μM against 50 protein kinases. See Supporting Information for more details.

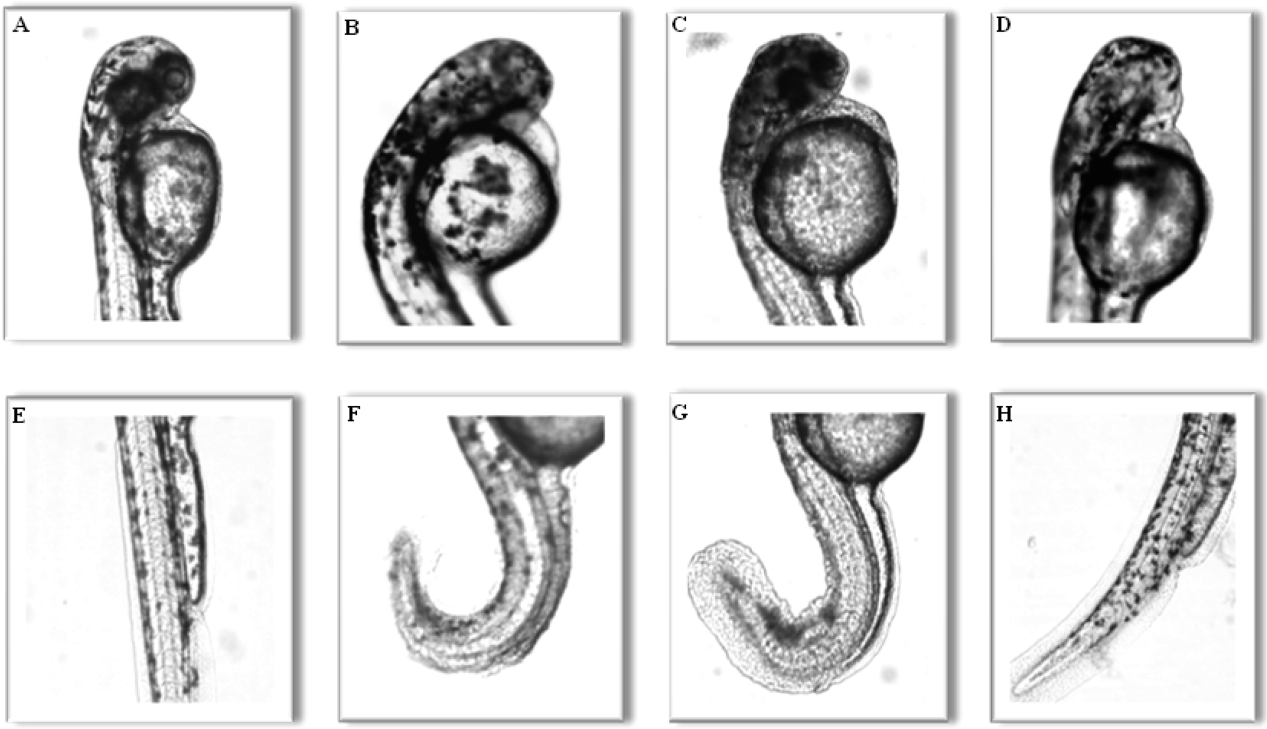

Figure 4. Effects on wild-type zebrafish embryos by compounds **14c**, **15a**, and **16a**. The embryos were collected and maintained in E2 medium at ~28 °C, compounds were added 5 hpf, and the phenotypes were compared at 44−48 hpf. (A,E) Head and tail of control embryos: DMSO (2%). (B,F) Head and tail of embryos treated with **14c**. This compound causes the eyeless phenotype at 0.5 μM and a stunted and crooked tail at 1.0 μM. (C,G) Head and tail of embryos treated with **15a**. A fluffy eye pigmentation and a stunted and crooked tail were observed at 2.5 μM. (D,H) Head and tail of embryos treated with **16a**. This compound causes the eyeless phenotype and a crooked tail at 20 μM.

with EtOAc and successively washed with brine. The organic layer was dried over $MgSO_4$ and concentrated under reduced pressure to give **2A** (1.6 g, 89%) as a colorless solid. ^{1}H NMR (DMSO-d_6, 500 MHz): δ [ppm] = 3.81 (3H, s), 6.14 (2H, s), 7.03 (1H, d, J = 8.1 Hz), 7.38 (1H, d, J = 1.7 Hz), 7.57 (1H, dd, J = 8.1 Hz, J = 1.7 Hz). ^{13}C NMR (DMSO-d_6, 125 MHz): δ [ppm] = 52.0, 102.1, 108.2, 108.5, 123.4, 125.0, 147.6, 151.4, 165.6. EI-MS: m/z = 180 (M^+).

The following compound **2B** was prepared in a similar manner to that described for **2A**.

Methyl 2,3-Dihydrobenzo[*b*][1,4]dioxine-6-carboxylate (2B). Yield 83%, colorless solid. ^{1}H NMR (DMSO-d_6, 500 MHz): δ [ppm] = 3.80 (3H, s), 4.19 (2H, m), 4.23 (2H, m), 6.80 (1H, m), 7.47 (2H, m). ^{13}C NMR (DMSO-d_6, 125 MHz): δ [ppm] = 50.5, 62.7, 63.2, 115.7, 117.6, 122.0, 141.7, 146.4, 165.2. EI-MS: m/z 194 (M^+).

Benzo[*d*][1,3]dioxole-5-carbohydrazide (3A). To a solution of **2A** (1.08 g, 6.0 mmol) in EtOH (30 mL) was added hydrazine hydrate (2.91 mL, 60 mmol), and the mixture was heated at reflux for 2 days. After cooling to room temperature, pure crystals are formed, collected by filtration, and washed several times with EtOH to give compound **3A** (0.72 g, 67%) as a colorless solid. ^{1}H NMR (DMSO-d_6, 500 MHz): δ [ppm] = 4.42 (2H, s), 6.07 (2H, s), 6.96 (1H, d, J = 8.1 Hz), 7.35 (1H, d, J = 1.7 Hz), 7.42 (1H, dd, J = 8.1 Hz, J = 1.7 Hz), 9.59 (1H, s). ^{13}C NMR (DMSO-d_6, 125 MHz): δ [ppm] = 101.5, 106.9, 107.8, 121.8, 127.2, 147.2, 149.5, 165.2. EI-MS: m/z = 180 (M^+).

Compound **3B** was prepared in a similar manner to that described for **3A**.

2,3-Dihydrobenzo[*b*][1,4]dioxine-6-carbohydrazide (3B). Yield 75%, light-yellow solid. ^{1}H NMR (methanol-d_4, 500 MHz): δ [ppm] = 4.28 (2H, m), 4.30 (2H, m), 6.89 (1H, d, J = 8.3 Hz), 7.30 (1H, dd, J = 8.3 Hz, J = 2.1 Hz), 7.33 (1H, d, J = 2.1 Hz), NH signals were not observed. ^{13}C NMR (methanol-d_4, 125 MHz): δ [ppm] = 65.9, 66.3, 117.9, 118.6, 121.9, 127.5, 145.2, 148.6, 169.6. EI-MS: m/z 194 (M^+).

5-(Benzo[*d*][1,3]dioxol-5-yl)-1,3,4-oxadiazole-2-thiol (4A). To a solution of **3A** (535 mg, 3.00 mmol) in EtOH (5 mL) were added carbon disulfide (397 μL, 6.60 mmol) and NEt_3 (469 μL, 3.30 mmol), and the mixture was heated at reflux overnight. The reaction mixture was diluted with EtOAc, and the organic layer was washed with 0.1 N HCl and brine and dried over Na_2SO_4. The solvent was evaporated under reduced pressure, and the obtained residue was recrystallized from cyclohexane/EtOAc to give **4A** (521 mg, 79%) as a pale-yellow solid. ^{1}H NMR (DMSO-d_6, 500 MHz): δ [ppm] = 6.14 (2H, s), 7.10 (1H, d, J = 8.1 Hz), 7.33 (1H, d, J = 1.6 Hz), 7.42 (1H, dd, J = 8.1 Hz, J = 1.6 Hz), SH signal was not observed. ^{13}C NMR (DMSO-d_6, 125 MHz): δ [ppm] = 102.1, 105.6, 109.1, 116.1, 121.5, 148.1, 150.6, 160.3, 177.2. EI-MS: m/z = 222 (M^+).

The compounds **4B−C** were prepared in a similar manner to that described for **4A**.

5-(2,3-Dihydrobenzo[*b*][1,4]dioxin-6-yl)-1,3,4-oxadiazole-2-thiol (4B). Yield 89%, light-brown solid. ^{1}H NMR (DMSO-d_6, 500 MHz): δ [ppm] = 4.32 (2H, m), 4.34 (2H, m), 7.05 (1H, d, J = 8.4 Hz), 7.30 (1H, d, J = 2.0 Hz), 7.36 (1H, dd, J = 8.4 Hz, J = 2.0 Hz), SH signal was not observed. ^{13}C NMR (DMSO-d_6, 125 MHz): δ [ppm] = 64.4, 64.8, 115.0, 115.7, 118.6, 120.0, 144.2, 147.3, 160.6, 177.6. EI-MS: m/z = 236 (M^+).

5-(Pyridin-4-yl)-1,3,4-oxadiazole-2-thiol (4C). Yield 83%, yellow solid. ^{1}H NMR (DMSO-d_6, 500 MHz): δ [ppm] = 7.81 (2H, dd, J = 4.4 Hz, J = 1.6 Hz), 8.81 (2H, dd, J = 4.4 Hz, J = 1.6 Hz), SH signal was not observed. ^{13}C NMR (DMSO-d_6, 125 MHz): δ [ppm] = 119.6, 129.7, 150.8, 158.7, 177.8. EI-MS: m/z = 179 (M^+).

3-((5-Benzo[*d*][1,3]dioxol-5-yl)-1,3,4-oxadiazol-2-ylthio)-methyl)benzonitrile (5a). To a solution of **4A** (55 mg, 0.25 mmol) and 1 N NaOH (0.25 mL, 0.25 mmol) in DMF (1 mL) was added 1-(bromomethyl)-3-methoxybenzene (75 mg, 0.38 mmol) at room temperature, and the mixture was stirred for 5 h. The precipitate formed was collected by filtration and washed once with less DMF (~1 mL) and thereafter several times with EtOH to give compound **5a** (55 mg, 64%) as a brown solid. ^{1}H NMR (DMSO-d_6, 500 MHz): δ [ppm] = 4.61 (2H, s), 6.16 (2H, s), 7.10 (1H, d, J = 8.1 Hz), 7.41 (1H, d, J = 1.4 Hz), 7.47 (1H, dd, J = 8.1 Hz, J = 1.5 Hz), 7.57 (1H, t,

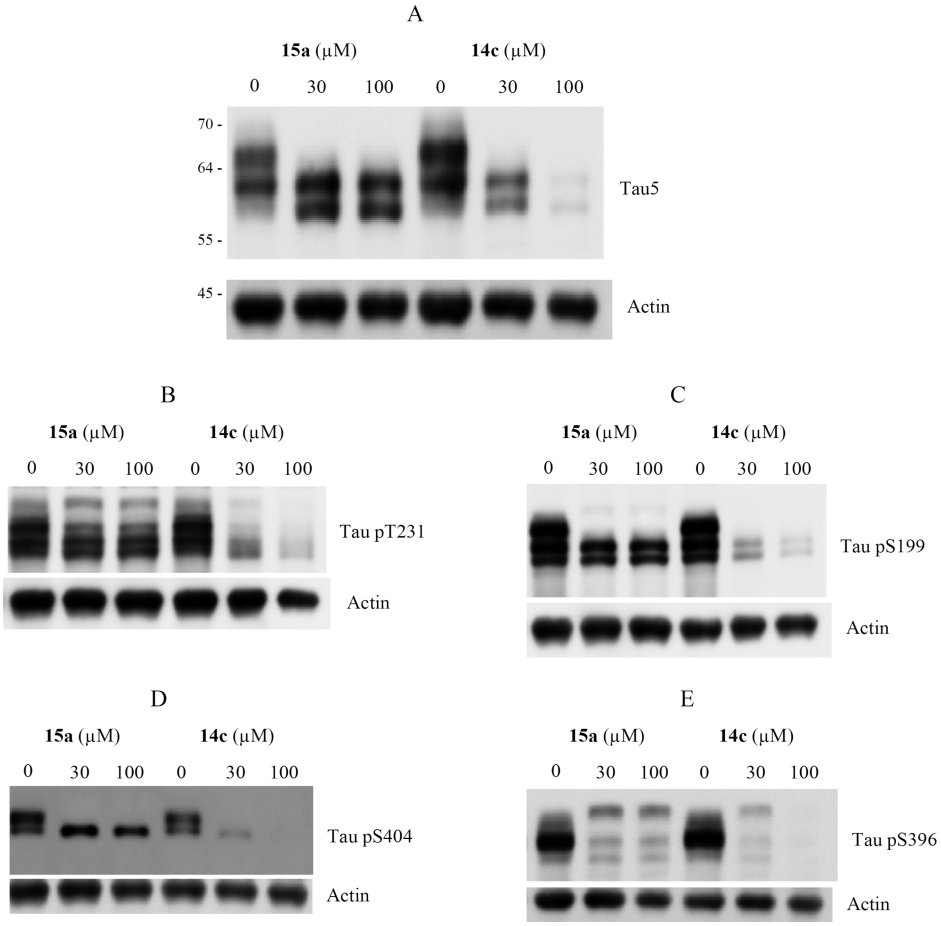

Figure 5. Western blotting for protein Tau.P301L expressed in stably transfected SH-SY5Y neuorblastoma cells, untreated (lanes marked 0) or treated for 6 h with compounds **14c** or **15a** (lanes marked 30 and 100 μM). Total protein tau was detected with antibody Tau5 (A). Phospho-epitopes on protein tau were detected with specific antibodies (B−E). Experiments were performed in triplicate, and representative blots are shown. Similar observations were obtained after 24 h of incubation. Note that compound **14c** specifically decreases the total concentration of protein tau, while levels of the internal marker (actin) remain unchanged.

J = 7.7 Hz), 7.76 (1H, d, J = 7.7 Hz), 7.84 (1H, d, J = 7.8 Hz), 7.96 (1H, s). ^{13}C NMR (DMSO-d_6, 125 MHz): δ [ppm] = 34.7, 102.1, 106.1, 109.1, 111.4, 116.6, 118.5, 121.7, 129.8, 131.4, 132.6, 133.9, 138.8, 148.1, 150.4, 162.2, 165.2. HPLC: 98%; t_R 7.21 min. EI-MS: m/z = 337 (M^+).

The compounds **5b−c**, **6a−c**, and **7a−c** were prepared in a similar manner to that described for **5a**. Note: Compounds which did not precipitate in solution were purified as follows. The reaction mixture was diluted with EtOAc and the organic layer was washed with water and brine, dried over $MgSO_4$, and concentrated in vacuo. The residue was purified by silica gel column chromatography (cyclohexane/EtOAc).

4-((5-Benzo[*d*][1,3]dioxol-5-yl)-1,3,4-oxadiazol-2-ylthio)-methyl)benzonitrile (5b). Yield 67%, brown solid. ^{1}H NMR (DMSO-d_6, 500 MHz): δ [ppm] = 4.64 (2H, s), 6.16 (2H, s), 7.11 (1H, d, J = 8.1 Hz), 7.42 (1H, d, J = 1.6 Hz), 7.48 (1H, dd, J = 8.1 Hz, J = 1.7 Hz) 7.68 (2H, d, J = 8.3 Hz), 7.82 (2H, d, J = 8.3 Hz). ^{13}C NMR (DMSO-d_6, 125 MHz): δ [ppm] = 35.2, 102.1, 106.1, 109.1, 110.4, 116.5, 118.6, 121.7, 130.0, 132.4, 142.8, 148.1, 150.5, 162.2, 165.2. HPLC: 95%; t_R 7.09 min. EI-MS: m/z = 337 (M^+).

Methyl 4-((5-(Benzo[*d*][1,3]dioxol-5-yl)-1,3,4-oxadiazol-2-ylthio)methyl Benzoate (5c). Yield 71%, pale-brown solid. ^{1}H NMR (DMSO-d_6, 500 MHz): δ [ppm] = 3.82 (3H, s), 4.63 (2H, s), 6.15 (2H, s), 7.10 (1H, d, J = 8.1 Hz), 7.41 (1H, d, J = 1.7 Hz), 7.48 (1H, dd, J = 8.1 Hz, J = 1.7 Hz), 7.62 (2H, d, J = 8.4 Hz), 7.92 (2H, d, J = 8.4 Hz). ^{13}C NMR (DMSO-d_6, 125 MHz): δ [ppm] = 35.4, 52.2, 102.2, 106.1, 109.2, 116.6, 121.7, 128.8, 129.4, 142.4, 148.1, 150.4, 162.3, 165.1, 165.9. HPLC: 96%; t_R 7.61 min. EI-MS: m/z = 370 (M^+).

3-((5-(2,3-Dihydrobenzo[*b*][1,4]dioxin-6-yl)-1,3,4-oxadiazol-2ylthio)methyl)benzonitrile (6a). Yield 73%, light-brown solid. ^{1}H NMR (DMSO-d_6, 500 MHz): δ [ppm] = 4.31 (2H, m), 4.34 (2H, m), 4.61 (2H, s), 7.05 (1H, d, J = 8.4 Hz), 7.39 (1H, d, J = 2.0 Hz), 7.42 (1H, dd, J = 8.4 Hz, J = 2.1 Hz), 7.57 (1H, t, J = 7.8 Hz), 7.77 (1H, dt, J = 7.8 Hz, J = 1.3 Hz), 7.84 (1H, dt, J = 7.8 Hz, J = 1.1 Hz), 7.96 (1H, t, J = 1.3 Hz). ^{13}C NMR (DMSO-d_6, 125 MHz): δ [ppm] = 35.2, 64.5, 64.7, 111.8, 115.5, 116.3, 118.5, 118.9, 120.4, 130.1, 131.8, 133.0, 134.4, 139.3, 144.2, 147.1, 162.7, 165.5. HPLC: 99%; t_R 7.53 min. EI-MS: m/z = 351 (M^+).

4-((5-(2,3-Dihydrobenzo[*b*][1,4]dioxin-6-yl)-1,3,4-oxadiazol-2-ylthio)methyl)benzonitrile (6b). Yield 56%, brown solid. ^{1}H NMR (DMSO-d_6, 500 MHz): δ [ppm] = 4.31 (2H, m), 4.34 (2H, m), 4.63 (2H, s), 7.05 (1H, d, J = 8.4 Hz), 7.37 (1H, d, J = 2.0 Hz), 7.41 (1H, dd, J = 8.4 Hz, J = 2.0 Hz), 7.67 (2H, d, J = 8.3 Hz), 7.81 (2H, d, J = 8.3 Hz). ^{13}C NMR (DMSO-d_6, 125 MHz): δ [ppm] = 35.3, 64.0, 64.4, 110.4, 115.0, 115.8, 118.2, 118.6, 119.9, 130.0, 132.4, 142.8, 143.8, 146.7, 162.2, 165.0. HPLC: 95%; t_R 7.49 min. EI-MS: m/z = 351 (M^+).

Methyl 4-((5-(2,3-Dihydrobenzo[*b*][1,4]dioxin-6-yl)-1,3,4-oxadiazol-2-ylthio)methyl) Benzoate (6c). Yield 49%, purple solid. ^{1}H NMR (DMSO-d_6, 500 MHz): δ [ppm] = 3.89 (3H, s), 4.36 (2H, m), 4.39 (2H, m), 4.67 (2H, s), 7.10 (1H, d, J = 8.4 Hz), 7.42 (1H, d, J = 2.0 Hz), 7.47 (1H, dd, J = 8.4 Hz, J = 2.0 Hz), 7.67 (2H, d, J = 8.3 Hz), 7.97 (2H, d, J = 8.3 Hz). ^{13}C NMR (DMSO-d_6, 125 MHz): δ [ppm] = 35.4, 52.1, 64.0, 64.4, 115.0, 115.8, 118.1, 120.0, 128.9, 129.4, 142.4, 143.8, 146.7, 162.3, 165.0, 165.8. HPLC: 99%; t_R 7.66 min.

EI-MS: m/z = 384 (M^+). HRMS (EI): m/z calcd for $C_{19}H_{16}N_2O_5S$ 384.0780, found 384.0809.

3-((5-(Pyridin-4-yl)-1,3,4-oxadiazol-2-ylthio)methyl)-benzonitrile (7a). Yield 41%, yellow solid. ^{1}H NMR (DMSO-d_6, 500 MHz): δ [ppm] = 4.66 (2H, s), 7.58 (1H, t, J = 7.8 Hz), 7.78 (1H, dt, J = 7.7 Hz, J = 1.3 Hz), 7.86 (1H, t, J = 1.2 Hz), 7.88 (2H, dd, J = 4.4 Hz, J = 1.6 Hz), 7.99 (1H, t, J = 1.4 Hz), 8.82 (2H, dd, J = 4.4 Hz, J = 1.6 Hz). ^{13}C NMR (DMSO-d_6, 125 MHz): δ [ppm] = 34.8, 111.4, 118.5, 120.0, 129.8, 130.0, 131.5, 132.7, 134.0, 138.6, 150.9, 163.8, 164.4. HPLC: 96%; t_R 4.51 min. EI-MS: m/z = 294 (M^+).

4-((5-(Pyridin-4-yl)-1,3,4-oxadiazol-2-ylthio)methyl)-benzonitrile (7b). Yield 77%, pale-yellow solid. ^{1}H NMR (DMSO-d_6, 500 MHz): δ [ppm] = 4.69 (2H, s), 7.71 (2H, d, J = 8.2 Hz), 7.83 (2H, d, J = 8.2 Hz), 7.88 (2H, dd, J = 4.4 Hz, J = 1.6 Hz), 8.82 (2H, dd, J = 4.5 Hz, J = 1.5 Hz). ^{13}C NMR (DMSO-d_6, 125 MHz): δ [ppm] = 35.2, 110.5, 118.6, 120.0, 130.0, 130.1, 132.4, 142.6, 150.8, 163.9, 164.4. HPLC: 95%; t_R 4.51 min. EI-MS: m/z = 294 (M^+).

2-(Benzylthio)-5-(pyridin-4-yl)-1,3,4-oxadiazole (7c). Yield 79%, light-yellow solid. ^{1}H NMR (DMSO-d_6, 500 MHz): δ [ppm] = 4.62 (2H, s), 7.30 (1H, m), 7.36 (2H, m), 7.50 (2H, m), 7.90 (2H, dd, J = 4.4 Hz, J = 1.6 Hz), 8.82 (2H, dd, J = 4.4 Hz, 1.6 Hz). ^{13}C NMR (DMSO-d_6, 125 MHz): δ [ppm] = 35.8, 120.0, 127.8, 128.6, 129.1, 130.0, 136.4, 150.8, 163.6, 164.7. HPLC: 100%; t_R 4.89 min. EI-MS: m/z = 269 (M^+).

2-(3-Iodobenzylthio)-5-(pyridin-4-yl)-1,3,4-oxadiazole (7d). **7d** was used as reference. It is commercially available from Calbiochem (361541 GSK-3β Inhibitor II; CAS number, 478482-75-6).

4-((5-(Benzo[*d*][1,3]dioxol-5-yl)-1,3,4-oxadiazol-2-ylthio)-methyl)benzoic Acid (8a). Methyl 4-((5-(benzo[*d*][1,3]dioxol-5-yl)-1,3,4-oxadiazol-2-ylthio)methyl benzoate **5c** (300 mg, 0.81 mmol) was added in 5 mL of a 2 N lithium hydroxide−tetrahydrofuran solution. The reaction mixture was stirred overnight at 60 °C under an argon atmosphere. The reaction mixture was diluted with water and neutralized with 1 N HCl. Afterward, EtOAc was added and the organic layer was washed with water and brine, dried over $MgSO_4$, and concentrated in vacuo to give **8a** (239 mg, 83%) as a rose solid. ^{1}H NMR (DMSO-d_6, 500 MHz): δ [ppm] = 4.56 (2H, s), 6.08 (2H, s), 7.04 (1H, d, J = 8.1 Hz), 7.35 (1H, d, J = 1.6 Hz), 7.43 (1H, dd, J = 8.1 Hz, J = 1.7 Hz), 7.53 (2H, d, J = 8.2 Hz), 7.84 (2H, d, J = 8.2 Hz), 12.8 (1H, s, br). ^{13}C NMR (DMSO-d_6, 125 MHz): δ [ppm] = 35.4, 102.1, 106.1, 109.1, 116.6, 121.7, 129.1, 129.5, 130.4, 141.7, 148.1, 150.4, 162.4, 165.1, 166.9. HPLC: 99%; t_R 6.15 min. EI-MS: m/z = 356 (M^+).

Compound **9a** was prepared in a similar manner to that described for **8a**.

Methyl 4-((5-(2,3-Dihydrobenzo[*b*][1,4]dioxin-6-yl)-1,3,4-oxadiazol-2-ylthio)methyl)benzoic Acid (9a). Yield 91%, colorless solid. ^{1}H NMR (DMSO-d_6, 500 MHz): δ [ppm] = 4.31 (2H, m), 4.34 (2H, m), 4.62 (2H, s), 7.05 (1H, d, J = 8.4 Hz), 7.38 (1H, d, J = 2.0 Hz), 7.43 (1H, dd, J = 8.4 Hz, J = 2.1 Hz), 7.59 (2H, d, J = 8.3 Hz), 7.91 (2H, d, J = 8.3 Hz), 12.95 (1H, s). ^{13}C NMR (DMSO-d_6, 125 MHz): δ [ppm] = 35.4, 64.1, 64.4, 115.1, 115.7, 118.2, 119.8, 129.3, 129.5, 130.1, 141.9, 143.8, 146.7, 162.4, 165.0, 166.8. HPLC: 96%; t_R 6.22 min. EI-MS: m/z = 370 (M^+).

4-((5-(Benzo[*d*][1,3]dioxol-5-yl)-1,3,4-oxadiazol-2-ylthio)-methyl)-*N*-isobutylbenzamide (8c). A mixture of 4-((5-(benzo-[*d*][1,3]dioxol-5-yl)-1,3,4-oxadiazol-2-ylthio)methyl)benzoic acid **8a** (100 mg, 0.28 mmol) and thionyl chloride (30.5 μL, 0.42 mmol) was refluxed in dry toluene (1 mL) for about 2 h. Excess thionyl chloride was removed by repeated evaporation in vacuo with fresh dry toluene (3 × 1 mL). 2-Methylpropan-1-amine (27.8 μL, 0.28 mmol) and K_2CO_3 (38 mg, 0.28 mmol) were added in dry acetone (1 mL) cooled to 0 °C and stirred for 30 min. The crude acyl chloride was dissolved in dry acetone (0.5 mL) and added dropwise to the solution. After the addition was complete, stirring continued for 2 h. The reaction mixture was then diluted with water, extracted three times with EtOAc, and successively washed with brine. The organic layer was dried over $MgSO_4$ and concentrated under reduced pressure. The obtained residue was recrystallized from EtOH to give **8c** (90 mg, 81%) as a beige solid. ^{1}H NMR (DMSO-d_6, 500 MHz): δ [ppm] = 0.86 (6H, d, J = 6.7 Hz), 1.81 (1H, n, J = 6.7 Hz), 3.05 (2H, t, J = 6.7 Hz), 4.60 (2H, s), 6.16 (2H, s), 7.10 (1H, d, J = 8.1 Hz), 7.43 (1H, d, J = 1.6 Hz), 7.50 (1H, dd, J = 8.1 Hz, J = 1.7 Hz), 7.54 (2H, d, J = 8.2 Hz), 7.78 (2H, d, J = 8.3 Hz), 8.42 (1H, t, J = 5.7 Hz). ^{13}C NMR (DMSO-d_6, 125 MHz): δ [ppm] = 20.2, 28.0, 35.4, 46.6, 102.1, 106.1, 109.2, 116.6, 121.8, 127.5, 128.8, 134.1, 139.8, 148.1, 150.5, 162.4, 165.1, 165.8. HPLC: 95%; t_R 7.11 min. EI-MS: m/z = 411 (M^+).

The following compounds **8d** and **9c−e** were prepared in a similar manner to that described for **8c**.

4-((5-(Benzo[*d*][1,3]dioxol-5-yl)-1,3,4-oxadiazol-2-ylthio)-methyl)-*N*-(2,2-dimethoxyethyl)benzamide (8d). Yield 79%, light-yellow solid. ^{1}H NMR (DMSO-d_6, 500 MHz): δ [ppm] = 3.27 (6H, s), 3.33 (2H, br), 4.48 (1H, t, J = 5.6 Hz), 4.61 (2H, s), 6.16 (2H, s), 7.11 (1H, d, J = 8.1 Hz), 7.44 (1H, d, J = 1.7 Hz), 7.50 (1H, dd, J = 8.1 Hz, J = 1.7 Hz), 7.55 (2H, d, J = 8.1 Hz), 7.80 (2H, d, J = 8.1 Hz), 8.52 (1H, t, J = 5.7 Hz). ^{13}C NMR (DMSO-d_6, 125 MHz): δ [ppm] = 35.4, 41.1, 53.2, 101.8, 102.2, 106.2, 109.2, 116.6, 121.7, 127.5, 128.9, 133.5, 140.1, 148.1, 150.4, 162.4, 165.1, 166.0. HPLC: 95%; t_R 6.07 min. EI-MS: m/z = 443 (M^+).

4-((5-(2,3-Dihydrobenzo[*b*][1,4]dioxin-6-yl)-1,3,4-oxadiazol-2-ylthio)methyl)-*N*-isobutyl Benzamide (9c). Yield 92%, light-brown solid. ^{1}H NMR (DMSO-d_6, 500 MHz): δ [ppm] = 0.93 (6H, d, J = 6.7 Hz), 1.88 (1H, n, J = 6.7 Hz), 3.12 (2H, t, J = 6.6 Hz), 4.37 (2H, m), 4.39 (2H, m), 4.66 (2H, s), 7.10 (1H, d, J = 8.4 Hz), 7.45 (1H, d, J = 2.0 Hz), 7.48 (1H, dd, J = 8.4 Hz, J = 2.0 Hz), 7.60 (2H, d, J = 8.2 Hz), 7.85 (2H, d, J = 8.2 Hz), 8.46 (1H, t, J = 5.7 Hz). ^{13}C NMR (DMSO-d_6, 125 MHz): δ [ppm] = 20.2, 28.1, 35.4, 46.6, 64.1, 64.4, 115.0, 115.8, 118.1, 119.9, 127.4, 128.8, 134.1, 139.7, 143.8, 146.7, 162.4, 164.9, 165.8. HPLC: 96%; t_R 7.16 min. EI-MS: m/z = 425 (M^+).

4-((5-(2,3-Dihydrobenzo[*b*][1,4]dioxin-6-yl)-1,3,4-oxadiazol-2-ylthio)methyl)-*N*-(2,2-dimethoxy ethyl)benzamide (9d). Yield 84%, beige solid. ^{1}H NMR (DMSO-d_6, 500 MHz): δ [ppm] = 3.28 (6H, s), 3.35 (2H, d, J = 5.7 Hz), 4.31 (2H, m), 4.34 (2H, m), 4.50 (1H, t, J = 5.6 Hz), 4.61 (2H, s), 7.05 (1H, d, J = 8.3 Hz), 7.40 (1H, d, J = 2.0 Hz), 7.43 (1H, dd, J = 8.3 Hz, J = 2.0 Hz), 7.55 (2H, d, J = 8.2 Hz), 7.81 (2H, d, J = 8.2 Hz), 8.52 (1H, t, J = 5.8 Hz). ^{13}C NMR (DMSO-d_6, 125 MHz): δ [ppm] = 35.4, 41.1, 53.2, 64.0, 64.4, 101.8, 115.0, 105.8, 108.2, 119.9, 127.4, 128.8, 133.5, 140.0, 143.8, 146.7, 162.4, 164.9, 165.9. HPLC: 95%; t_R 6.13 min. EI-MS: m/z = 457 (M^+).

***N*-Benzyl-4-((5-(2,3-dihydrobenzo[*b*][1,4]dioxin-6-yl)-1,3,4-oxadiazol-2-ylthio)methyl)benzamide (9e).** Yield 89%, beige solid. ^{1}H NMR (DMSO-d_6, 500 MHz): δ [ppm] = 4.31 (2H, m), 4.34 (2H, m), 4.47 (2H, d, J = 5.9 Hz), 4.62 (2H, s), 7.05 (1H, d, J = 8.4 Hz), 7.23 (1H, m), 7.32 (4H, m), 7.40 (1H, d, J = 2.0 Hz), 7.43 (1H, dd, J = 8.3 Hz, J = 2.0 Hz), 7.56 (2H, d, J = 8.2 Hz), 7.86 (2H, d, J = 8.2 Hz), 9.01 (1H, t, J = 5.9 Hz). ^{13}C NMR (DMSO-d_6, 125 MHz): δ [ppm] = 35.4, 42.6, 64.1, 64.4, 115.1, 115.8, 118.3, 119.8, 126.7, 127.3, 127.5, 128.4, 128.8, 133.7, 139.6, 140.1, 143.8, 146.7, 162.4, 165.0, 165.8. HPLC: 95%; t_R 7.66 min. EI-MS: m/z = 459 (M^+).

2-(4-(1*H*-Tetrazol-5-yl)benzylthio)-5-(benzo[*d*][1,3]dioxol-5-yl)-1,3,4-oxadiazole (8e). 4-((5-Benzo[*d*][1,3]dioxol-5-yl)-1,3,4-oxadiazol-2-ylthio)methyl)benzonitrile **5b** (34 mg, 0.10 mmol), NaN_3 (78 mg, 1.20 mmol), and NH_4Cl (64 mg, 1.20 mmol) were added to 1 mL of DMF and stirred for 5 h at 100 °C under microwave irradiation. After cooling to room temperature, the reaction solution was added to water (2−3 mL), acidified with 2 N HCl, and extracted three times with ethyl acetate. The combined organic layers were dried over Na_2SO_4, filtered, and the solvent evaporated off to provide **8e** (25 mg, 67%) as a beige solid. ^{1}H NMR (DMSO-d_6, 500 MHz): δ [ppm] = 4.65 (2H, s), 6.15 (2H, s), 7.11 (1H, d, J = 8.1 Hz), 7.43 (1H, d, J = 1.6 Hz), 7.50 (1H, dd, J = 8.1 Hz, J = 1.7 Hz), 7.71 (2H, d, J = 8.3 Hz), 8.00 (2H, d, J = 8.3 Hz), NH signal was not observed. ^{13}C NMR (DMSO-d_6, 125 MHz): δ [ppm] = 35.4, 102.1, 105.0, 106.2, 108.9, 109.1, 116.6, 119.7, 121.7, 127.1, 130.0, 148.1, 150.4, 162.4, 165.1. HPLC: 96%; t_R 5.92 min. EI-MS: m/z = 380 (M^+).

Compound **9f** was prepared in a similar manner to that described for **8e**.

2-(4-(1*H*-Tetrazol-5-yl)benzylthio)-5-(2,3-dihydrobenzo[*d*]-[1,4]dioxin-5-yl)-1,3,4-oxadiazole (9f). Yield 79%, puce solid. ^{1}H NMR (DMSO-d_6, 500 MHz): δ [ppm] = 4.35 (2H, m), 4.38 (2H, m), 4.70 (2H, s), 7.10 (1H, d, J = 8.4 Hz), 7.43 (1H, d, J = 2.0 Hz),

7.47 (1H, dd, J = 8.4 Hz, J = 2.1 Hz), 7.75 (2H, d, J = 8.3 Hz), 8.05 (2H, d, J = 8.3 Hz), NH signal was not observed. ^{13}C NMR (DMSO-d_6, 125 MHz): δ [ppm] = 35.5, 64.0, 64.4, 115.0, 115.8, 118.2, 119.9, 123.6, 127.1, 130.0, 140.1, 143.8, 146.7, 162.4, 165.1. HPLC: 95%; t_R 6.01 min. EI-MS: m/z = 394 (M^+).

The following compounds **14a−d**, **15a−b**, and **16a** were prepared in a similar manner to that described for **5a**.

2-(Benzo[*d*][1,3]dioxol-5-yl)-5-(biphenyl-4-ylmethylthio)-1,3,4-oxadiazole (14a). Yield 75%, beige solid. ^{1}H NMR (DMSO-d_6, 500 MHz): δ [ppm] = 4.55 (2H, s), 6.08 (2H, s), 7.04 (1H, d, J = 8.1 Hz), 7.28 (1H, m), 7.38 (3H, m), 7.45 (1H, dd, J = 8.1 Hz, J = 1.7 Hz), 7.48 (2H, d, J = 8.3 Hz), 7.58 (4H, m). ^{13}C NMR (DMSO-d_6, 125 MHz): δ [ppm] = 35.6, 102.1, 106.2, 109.1, 116.6, 121.7, 126.6, 126.8, 127.6, 128.9, 129.7, 135.8, 139.6, 148.1, 150.5, 162.6, 165.1. HPLC: 95%; t_R 9.12 min. EI-MS: m/z = 388 (M^+).

4′-((5-(Benzo[*d*][1,3]dioxol-5-yl)-1,3,4-oxadiazol-2-ylthio)-methyl)biphenyl-2-carbonitrile (14b). Yield 71%, brown solid. ^{1}H NMR (DMSO-d_6, 500 MHz): δ [ppm] = 4.66 (2H, s), 6.15 (2H, s), 7.11 (1H, d, J = 8.1 Hz), 7.45 (1H, d, J = 1.7 Hz), 7.51 (1H, dd, J = 8.1 Hz, J = 1.7 Hz), 7.57 (2H, d, J = 8.2 Hz), 7.65 (4H, m), 7.96 (1H, dd, J = 8.5 Hz, J = 2.3 Hz). ^{13}C NMR (DMSO-d_6, 125 MHz): δ [ppm] = 35.5, 102.1, 106.1, 109.1, 111.5, 111.6, 116.6, 117.3, 117.4, 120.3, 120.5, 121.0, 121.2, 121.7, 129.0, 129.4, 132.3, 132.4, 136.2, 137.5, 140.8, 140.9, 148.1, 150.4, 159.9, 161.9, 162.6, 165.1. HPLC: 95%; t_R 8.77 min. EI-MS: m/z = 431 (M^+). HRMS (EI): m/z calcd for $C_{23}H_{14}N_3O_3FS$ 431.0740, found 431.0728.

4-((5-(Benzo[*d*][1,3]dioxol-5-yl)-1,3,4-oxadiazol-2-ylthio)-methyl)-4-fluorobiphenyl-2-carbonitrile (14c). Yield 69%, gray solid. ^{1}H NMR (DMSO-d_6, 500 MHz): δ [ppm] = 4.66 (2H, s), 6.16 (2H, s), 7.11 (1H, d, J = 8.1 Hz), 7.45 (1H, d, J = 1.7 Hz), 7.51 (1H, dd, J = 8.1 Hz, J = 1.7 Hz), 7.56 (2H, d, J = 8.2 Hz), 7.65 (4H, m), 7.78 (1H, td, J = 7.7 Hz, J = 1.3 Hz), 7.95 (1H, dd, J = 7.7 Hz, J = 0.9 Hz). ^{13}C NMR (DMSO-d_6, 125 MHz): δ [ppm] = 35.5, 102.1, 106.1, 109.1, 110.1, 116.6, 118.5, 121.7, 128.3, 128.9, 129.4, 130.1, 133.5, 133.8, 137.2, 137.4, 140.0, 148.1, 150.4, 162.6, 165.1. HPLC: 96%; t_R 8.36 min. EI-MS: m/z = 413 (M^+). HRMS (EI): m/z calcd for $C_{23}H_{15}N_3O_3S$ 413.0835, found 413.0804.

4′-((5-(Benzo[*d*][1,3]dioxol-5-yl)-1,3,4-oxadiazol-2-ylthio)-methyl)biphenyl-4-carbonitrile (14d). Yield 51%, gray−brown solid. ^{1}H NMR (DMSO-d_6, 500 MHz): δ [ppm] = 4.63 (2H, s), 6.15 (2H, s), 7.10 (1H, d, J = 8.1 Hz), 7.43 (1H, d, J = 1.7 Hz), 7.51 (1H, dd, J = 8.1 Hz, J = 1.7 Hz), 7.61 (2H, d, J = 8.3 Hz), 7.73 (2H, d, J = 8.3 Hz), 7.87 (2H, d, J = 8.6 Hz), 7.91 (2H, d, J = 8.6 Hz). ^{13}C NMR (DMSO-d_6, 125 MHz): δ [ppm] = 35.9, 102.6, 106.6, 109.6, 110.6, 117.1, 119.3, 122.2, 127.7, 128.0, 130.3, 133.3, 138.0, 138.1, 144.5, 148.6, 150.9, 163.0, 165.5. HPLC: 97%; t_R 8.77 min. EI-MS: m/z = 413 (M^+). HRMS (EI): m/z calcd for $C_{23}H_{15}N_3O_3S$ 413.0835, found 413.0825.

4-((5-(2,3-Dihydrobenzo[*b*][1,4]dioxin-6-yl)-[1,3,4]oxadiazol-2-ylthio)methyl)biphenyl-2-carbonitrile (15a). Yield 74%, colorless solid. ^{1}H NMR (DMSO-d_6, 500 MHz): δ [ppm] = 4.31 (2H, m), 4.34 (2H, m), 4.65 (2H, s), 7.05 (1H, d, J = 8.4 Hz), 7.41 (1H, d, J = 2.0 Hz), 7.44 (1H, dd, J = 8.4 Hz, J = 2.0 Hz), 7.60 (6H, m), 7.79 (1H, td, J = 7.7 Hz, J = 1.2 Hz), 7.95 (1H, dd, J = 7.7 Hz, J = 0.9 Hz). ^{13}C NMR (DMSO-d_6, 125 MHz): δ [ppm] = 35.9, 64.4, 64.8, 110.5, 115.4, 116.3, 118.5, 118.8, 120.3, 128.6, 129.3, 129.7, 130.5, 133.8, 134.2, 137.5, 137.8, 144.1, 144.3, 147.1, 163.0, 165.3. HPLC: 100%; t_R 8.39 min. EI-MS: m/z 427 (M^+). HRMS (EI): m/z calcd for $C_{24}H_{17}N_3O_3S$ 427.0991, found 427.0962.

4′-((5-(2,3-Dihydrobenzo[*b*][1,4]dioxin-6-yl)-1,3,4-oxadiazol-2-ylthio)methyl)-4-fluorobiphenyl-2-carbonitrile (15b). Yield 29%, light-yellow solid. ^{1}H NMR (DMSO-d_6, 500 MHz): δ [ppm] = 4.32 (2H, m), 4.34 (2H, m) 4.65 (2H, s), 7.05 (1H, d, J = 8.4 Hz), 7.40 (1H, d, J = 2.1 Hz), 7.45 (1H, dd, J = 8.4 Hz, J = 2.1 Hz), 7.56 (2H, d, J = 8.2 Hz), 7.63 (2H, d, J = 8.2 Hz), 7.68 (2H, m), 7.97 (1H, dd, J = 9.0 Hz, J = 1.9 Hz). HPLC: 95%; t_R 8.76 min. EI-MS: m/z = 445 (M^+). HRMS (EI): m/z calcd for $C_{24}H_{16}N_3O_3FS$ 445.0897, found 445.0890.

4-((5-(Pyridine-4-yl)-1,3,4-oxadiazol-2-ylthio)methyl)-biphenyl-2-carbonitrile (16a). Yield 53%, colorless solid. ^{1}H NMR (DMSO-d_6, 500 MHz): δ [ppm] = 4.71 (2H, s), 7.58 (3H, m), 7.62 (1H, d, J = 7.7 Hz), 7.68 (2H, d, J = 8.1 Hz), 7.78 (1H, t, J = 7.7 Hz), 7.91 (2H, d, J = 4.1 Hz), 7.95 (1H, d, J = 7.7 Hz), 8.85 (2H, s, br). ^{13}C NMR (DMSO-d_6, 125 MHz): δ [ppm] = 35.4, 110.1, 118.5, 120.1, 128.2, 128.9, 129.4, 130.0, 130.1, 133.5, 133.7, 137.2, 137.3, 143.9, 150.8, 163.8, 164.8. HPLC: 99%; t_R 6.63 min. EI-MS: m/z = 370 (M^+). HRMS (EI): m/z calcd for $C_{21}H_{14}N_4OS$ 370.0889, found 370.0926.

Methyl 3,4-Dihydroxybenzoate (18). To a stirred solution of 3,4-dihydroxybenzoic acid (2.0 g, 13 mmol) in MeOH (25 mL) was added $SOCl_2$ (1.88 mL, 26 mmol) dropwise over 1 h at 0 °C. The solution was further stirred 12 h at 50 °C. The mixture was cooled to room temperature and diluted with water (30 mL). MeOH was evaporated and the pH adjusted to ∼6 with aqueous $NaHCO_3$. The mixture was extracted three times with EtOAc and successively washed with brine. The organic layer was dried over $MgSO_4$ and concentrated under reduced pressure to give **18** (2.1 g, 97%) as a colorless solid. ^{1}H NMR (DMSO-d_6, 500 MHz): δ [ppm] = 3.75 (3H, s), 6.80 (1H, d, J = 8.2 Hz), 7.31 (1H, dd, J = 8.2 Hz, J = 2.1 Hz), 7.35 (1H, d, J = 2.1 Hz), 9.35 (1H, s), 9.75 (1H, s). ^{13}C NMR (DMSO-d_6, 125 MHz): δ [ppm] = 51.5, 115.3, 116.2, 120.4, 121.7, 145.0, 150.4, 166.1. EI-MS: m/z = 168 (M^+).

Methyl 3-(Hydroxymethyl)-2,3-dihydrobenzo[*b*][1,4]-dioxine-6-carboxylate (19a). Methyl 3,4-dihydroxybenzoate **18** (0.8 g, 4.75 mmol) and K_2CO_3 (0.65 g, 4.75 mmol) were taken in dry acetone (10 mL) and stirred for 15 min at room temperature. Afterward, the solution was treated with epibromohydrin (0.40 mL, 4.75 mmol) and stirred overnight at 70 °C. The reaction mixture was diluted with water and extracted with EtOAc. The organic layer was washed with brine and dried over Na_2SO_4. The solvent was evaporated under reduced pressure and the crude product purified by silica gel column chromatography (DCM/EtOAc, 4:1) to give **19a** (1.01 g, 95%) as a colorless oil. ^{1}H NMR (DMSO-d_6, 500 MHz): δ [ppm] = 3.64 (2H, m), 3.80 (3H, s), 4.10 (1H, m), 4.20 (1H, m), 4.41 (1H, dd, J = 11.4 Hz, J = 2.3 Hz), 5.10 (1H, t, J = 5.7 Hz), 6.98 (1H, d, J = 8.4 Hz), 7.41 (1H, d, J = 2.0 Hz), 7.46 (1H, dd, J = 8.4 Hz, J = 2.0 Hz). ^{13}C NMR (DMSO-d_6, 125 MHz): δ [ppm] = 51.9, 59.7, 65.4, 73.6, 117.0, 117.9, 122.6, 122.7, 142.8, 147.4, 165.6. EI-MS: m/z = 224 (M^+).

Note: Alternatively (R/S)-(±)-glycidyl tosylate can be used to obtain compound **19a**. For more details see the synthesis of compound **19b−c**.

Methyl 3-(Methoxymethyl)-2,3-dihydrobenzo[*b*][1,4]-dioxine-6-carboxylate (20a). To a suspension of NaH (115 mg, 4.81 mmol) in 5 mL of anhydrous THF was added methyl 3-(hydroxymethyl)-2,3-dihydrobenzo[*b*][1,4]dioxine-6-carboxylate **19a** (900 mg, 4.01 mmol) at 0 °C. The mixture was stirred at room temperature for 30 min, followed by addition of methyl iodide (374 μL, 6.01 mmol). The reaction mixture was stirred at room temperature for 48 h, quenched with 10 mL of water, and extracted with ethyl acetate. The combined organic layer was dried over $MgSO_4$, the solvent was evaporated under reduced pressure, and the crude product purified by silica gel column chromatography (DCM/EtOAc, 20:1) to give **20a** (678 mg, 71%) as a colorless oil. ^{1}H NMR (DMSO-d_6, 500 MHz): δ [ppm] = 3.33 (3H, s), 3.60 (2H, m), 3.80 (3H, s), 4.09 (1H, m), 4.40 (2H, m), 6.99 (1H, m), 7.41 (1H, m), 7.47 (1H, m). ^{13}C NMR (DMSO-d_6, 125 MHz): δ [ppm] = 51.8, 58.7, 65.3, 70.3, 71.8, 117.0, 118.0, 122.7, 122.8, 142.6, 147.2, 165.5. EI-MS: m/z = 238 (M^+).

3-(Methoxymethyl)-2,3-dihydrobenzo[*b*][1,4]dioxine-6-carbohydrazide (21a). To a solution of **20a** (600 mg, 2.51 mmol) in EtOH (15 mL) was added hydrazine hydrate (731 μL, 15.06 mmol). and the mixture was heated at reflux for 2 days. After cooling to room temperature, the reaction mixture was diluted with water and extracted with EtOAc. The organic layer was washed with brine and dried over $MgSO_4$. The solvent was evaporated under reduced pressure and the crude product purified by silica gel column chromatography (MeOH/EtOAc, 1:10) to give **21a** (466 mg, 78%) as a colorless solid. ^{1}H NMR (DMSO-d_6, 500 MHz): δ [ppm] = 3.32 (3H, s), 3.59 (2H, m), 4.04 (1H, m), 4.36 (2H, m), 4.41 (2H, s), 6.92 (1H, d, J = 8.2 Hz), 7.35 (1H, dd, J = 8.2 Hz, J = 2.0 Hz), 7.37 (1H, d, J = 2.0 Hz), 9.52 (1H, s). ^{13}C NMR (DMSO-d_6, 125 MHz): δ [ppm] = 58.7, 65.1, 70.4, 71.8,

115.8, 116.6, 120.3, 126.5, 142.3, 145.3, 165.1. EI-MS: m/z = 238 (M^+).

Compound **22a** was prepared in a similar manner to that described for **4A**.

5-(3-(Methoxymethyl)-2,3-dihydrobenzo[*b*][1,4]dioxin-6-yl)-1,3,4-oxadiazole-2-thiol (22a). Yield 81%, orange solid. ^{1}H NMR (DMSO-d_6, 500 MHz): δ [ppm] = 3.32 (3H, s), 3.61 (2H, m), 4.10 (1H, m), 4.43 (2H, m), 7.07 (1H, m), 7.32 (1H, m), 7.37 (1H, m), 14.60 (1H, s). ^{13}C NMR (DMSO-d_6, 125 MHz): δ [ppm] = 58.7, 65.3, 70.3, 72.1, 114.6, 115.6, 118.0, 119.7, 143.4, 146.4, 160.1, 177.4. EI-MS: m/z = 280 (M^+).

Compound **23a** was prepared in a similar manner to that described for **5a**.

4′-((5-(3-(Methoxymethyl)-2,3-dihydrobenzo[*b*][1,4]dioxin-6-yl)-1,3,4-oxadiazol-2ylthio)methyl)biphenyl-2-carbonitrile (23a). Yield 88%, colorless solid. ^{1}H NMR (DMSO-d_6, 500 MHz): δ [ppm] = 3.33 (3H, s), 3.61 (2H, m), 4.10 (1H, m), 4.44 (2H, m), 4.66 (2H, s), 7.07 (1H, m), 7.45 (2H, m), 7.57 (3H, m), 7.63 (3H, m), 7.78 (1H, td, J = 7.6 Hz, J = 1.2 Hz), 7.95 (1H, dd, J = 7.7 Hz, J = 1.1 Hz). ^{13}C NMR (DMSO-d_6, 125 MHz): δ [ppm] = 35.4, 58.7, 65.2, 70.3, 72.0, 110.1, 115.1, 116.2, 118.0, 118.5, 119.9, 128.2, 128.8, 129.4, 130.1, 133.5, 133.8, 137.1, 137.4, 143.3, 143.9, 146.2, 162.6, 164.9. HPLC: 100%; t_R 8.59 min. EI-MS: m/z = 471 (M^+). HRMS (EI): m/z calcd for $C_{26}H_{21}N_3O_4S$ 471.1253, found 471.1264.

4′-((5-(3-(Hydroxymethyl)-2,3-dihydrobenzo[*b*][1,4]dioxin-6-yl)-1,3,4-oxadiazol-2-ylthio) methyl)biphenyl-2-carbonitrile (24a). To a solution of 4′-((5-(3-(methoxymethyl)-2,3-dihydrobenzo-[*b*][1,4]dioxin-6-yl)-1,3,4-oxadiazol-2ylthio)methyl)biphenyl-2-carbonitrile **23a** (400 mg, 0.85 mmol) in 10 mL of DCM was added 1 N solution of BBr_3 in hexane (850 μL, 0.85 mmol) under argon atmosphere at −78 °C. The reaction mixture was stirred at the same temperature for 1 h and allowed to warm to room temperature and further stirred for 24 h. After treatment with saturated $NaHCO_3$ solution, the reaction mixture was extracted with ethyl acetate. The combined organic layers were dried over $MgSO_4$ and concentrated under reduced pressure. The crude product was purified by silica gel column chromatography (cyclohexane/EtOAc, 1:2) to give compound **24a** (283 mg, 73%) as a light-yellow solid. ^{1}H NMR (DMSO-d_6, 500 MHz): δ [ppm] = 3.59 (1H, s, br), 3.64 (2H, m), 4.10 (1H, m), 4.24 (1H, m), 4.42 (1H, dd, J = 11.5 Hz, J = 2.2 Hz), 4.65 (2H, s) 7.06 (1H, d, J = 8.3 Hz), 7.43 (2H, m), 7.60 (6H, m), 7.78 (1H, td, J = 7.7 Hz, J = 1.2 Hz), 7.94 (1H, dd, J = 7.7 Hz, J = 1.0 Hz). ^{13}C NMR (DMSO-d_6, 125 MHz): δ [ppm] = 35.4, 59.6, 65.4, 73.7, 110.1, 115.1, 116.1, 117.9, 118.5, 119.8, 128.2, 128.8, 129.4, 130.1, 133.4, 133.8, 137.1, 137.4, 143.5, 144.0, 146.2, 162.6, 165.0. HPLC: 96%; t_R 7.39 min. EI-MS: m/z = 457(M^+).

(*R*)-Methyl 3-(Hydroxymethyl)-2,3-dihydrobenzo[*b*][1,4]-dioxine-6-carboxylate (19b). To a round-bottom flask equipped with magnetic stirring and a nitrogen inlet was added methyl-3,4-dihydroxybenzoate **18** (1.0 g, 6 mmol), (2*S*)-(+)-glycidyl tosylate (1.37 g, 6 mmol), K_2CO_3(0.99 g, 7.2 mmol), and DMF (15 mL). This mixture was heated to 60 °C for 5 h. The mixture was cooled to room temperature, diluted with water, and extracted with EtOAc. The organic layer was washed with brine and dried over Na_2SO_4. The solvent was evaporated under reduced pressure and the crude product purified by silica gel column chromatography (DCM/EtOAc, 4:1) to give **19b** (1.25 g, 93%) as a colorless oil. ^{1}H NMR (DMSO-d_6, 500 MHz): δ [ppm] = 3.64 (2H, m), 3.80 (3H, s), 4.10 (1H, m), 4.20 (1H, m), 4.41 (1H, dd, J = 11.4 Hz, J = 2.3 Hz), 5.08 (1H, t, J = 5.7 Hz), 6.98 (1H, d, J = 8.4 Hz), 7.41 (1H, d, J = 2.0 Hz), 7.46 (1H, dd, J = 8.4 Hz, J = 2.0 Hz). ^{13}C NMR (DMSO-d_6, 125 MHz): δ [ppm] = 51.9, 59.7, 65.5, 73.6, 117.0, 117.9, 122.6, 122.7, 142.8, 147.4, 165.6. HPLC: 96%; t_R 2.44 min. EI-MS: m/z = 224 (M^+).

Compound **19c** was prepared in a similar manner to that described for **19b**. (2*R*)-(−)-glycidyl tosylate was used instead of (2*S*)-(+)-glycidyl tosylate to obtain the *S*-isomer.

(*S*)-Methyl 3-(Hydroxymethyl)-2,3-dihydrobenzo[*b*][1,4]-dioxine-6-carboxylate (19c). Yield 89%, as a colorless oil. ^{1}H NMR (DMSO-d_6, 500 MHz): δ [ppm] = 3.64 (2H, m), 3.80 (3H, s), 4.10 (1H, m), 4.20 (1H, m), 4.41 (1H, dd, J = 11.4 Hz, J = 2.3 Hz), 5.10 (1H, s, br), 6.98 (1H, d, J = 8.4 Hz), 7.41 (1H, d, J = 2.0 Hz), 7.46 (1H, dd, J = 8.4 Hz, J = 2.0 Hz). ^{13}C NMR (DMSO-d_6, 125 MHz): δ [ppm] = 51.9, 59.7, 65.5, 73.6, 117.0, 117.9, 122.6, 122.7, 142.8, 147.4, 165.6. EI-MS: m/z = 224 (M^+).

Compounds **20b−c** were prepared in a similar manner to that described for **20a**.

(*R*)-Methyl 3-(Methoxymethyl)-2,3-dihydrobenzo[*b*][1,4]-dioxine-6-carboxylate (20b). Yield 68%, as a colorless oil. ^{1}H NMR (DMSO-d_6, 500 MHz): δ [ppm] = 3.33 (3H, s), 3.60 (2H, m), 3.81 (3H, s), 4.09 (1H, m), 4.40 (2H, m), 6.99 (1H, d, J = 8.4 Hz), 7.42 (1H, d, J = 2.0 Hz), 7.47 (1H, dd, J = 8.4 Hz, J = 2.0 Hz). ^{13}C NMR (DMSO-d_6, 125 MHz): δ [ppm] = 51.9, 58.7, 65.3, 70.3, 71.8, 117.1, 117.9, 122.8, 122.9, 142.6, 147.3, 165.6. EI-MS: m/z = 238 (M^+).

(*S*)-Methyl 3-(Methoxymethyl)-2,3-dihydrobenzo[*b*][1,4]-dioxine-6-carboxylate (20c). After extraction and evaporation of the solvent, compound **20c** was used without further purification.

Compounds **21b−c** were prepared in a similar manner to that described for **21a**.

(*R*)-3-(Methoxymethyl)-2,3-dihydrobenzo[*b*][1,4]dioxine-6-carbohydrazide (21b). Yield 87%, as a colorless solid. ^{1}H NMR (DMSO-d_6, 500 MHz): δ [ppm] = 3.32 (3H, s), 3.59 (2H, m), 4.04 (1H, m), 4.36 (2H, m), 4.41 (2H, s), 6.92 (1H, d, J = 8.3 Hz), 7.35 (1H, dd, J = 8.3 Hz, J = 2.0 Hz), 7.37 (1H, d, J = 2.0 Hz), 9.57 (1H, s). ^{13}C NMR (DMSO-d_6, 125 MHz): δ [ppm] = 58.7, 65.1, 70.4, 71.7, 115.8, 116.6, 120.4, 126.6, 142.3, 145.3, 165.1. EI-MS: m/z = 238 (M^+).

(*S*)-3-(Methoxymethyl)-2,3-dihydrobenzo[*b*][1,4]dioxine-6-carbohydrazide (21c). Yield 92%, as a colorless solid. ^{1}H NMR (DMSO-d_6, 500 MHz): δ [ppm] = 3.32 (3H, s), 3.59 (2H, m), 4.04 (1H, m), 4.36 (2H, m), 4.41 (2H, s), 6.92 (1H, d, J = 8.3 Hz), 7.36 (1H, dd, J = 8.3 Hz, J = 2.0 Hz), 7.37 (1H, d, J = 2.0 Hz), 9.57 (1H, s). ^{13}C NMR (DMSO-d_6, 125 MHz): δ [ppm] = 58.7, 65.1, 70.4, 71.8, 115.8, 116.6, 120.4, 126.6, 142.3, 145.3, 165.2. EI-MS: m/z = 238 (M^+).

Compounds **22b−c** were prepared in a similar manner to that described for **4A**.

(*R*)-5-(3-(Methoxymethyl)-2,3-dihydrobenzo[*b*][1,4]dioxin-6-yl)-1,3,4-oxadiazole-2-thiol (22b). Yield 91%, orange solid. ^{1}H NMR (DMSO-d_6, 500 MHz): δ [ppm] = 3.33 (3H, s), 3.61 (2H, m), 4.10 (1H, m), 4.42 (2H, m), 7.07 (1H, m), 7.31 (1H, m), 7.37 (1H, m), 14.62 (1H, s). ^{13}C NMR (DMSO-d_6, 125 MHz): δ [ppm] = 58.8, 65.3, 70.2, 72.1, 114.6, 115.6, 118.0, 119.7, 143.3, 146.4, 160.1, 177.2. EI-MS: m/z = 280 (M^+).

(*S*)-5-(3-(Methoxymethyl)-2,3-dihydrobenzo[*b*][1,4]dioxin-6-yl)-1,3,4-oxadiazole-2-thiol (22c). Yield 91%, orange solid. ^{1}H NMR (DMSO-d_6, 500 MHz): δ [ppm] = 3.33 (3H, s), 3.61 (2H, m), 4.09 (1H, m), 4.39 (2H, m), 7.02 (1H, m), 7.24 (1H, m), 7.30 (1H, m), SH signal was not observed. ^{13}C NMR (DMSO-d_6, 125 MHz): δ [ppm] = 58.6, 65.3, 70.0, 72.1, 114.6, 115.6, 117.7, 119.7, 143.3, 146.4, 160.1, 177.2. EI-MS: m/z = 280 (M^+).

Compounds **23b−c** were prepared in a similar manner to that described for **5a**.

(*R*)-4′-((5-(3-(Methoxymethyl)-2,3-dihydrobenzo[*b*][1,4]-dioxin-6-yl)-1,3,4-oxadiazol-2-ylthio) methyl)biphenyl-2-carbonitrile (23b). Yield 84%, colorless solid. ^{1}H NMR (DMSO-d_6, 500 MHz): δ [ppm] = 3.38 (3H, s), 3.66 (2H, m), 4.15 (1H, m), 4.47 (2H, m), 4.71 (2H, s), 7.13 (1H, m), 7.50 (2H, m), 7.65 (6H, m), 7.82 (1H, td, J = 7.7 Hz, J = 1.3 Hz), 8.00 (1H, dd, J = 7.7 Hz, J = 0.9 Hz). ^{13}C NMR (DMSO-d_6, 125 MHz): δ [ppm] = 35.4, 58.7, 65.2, 70.4, 72.0, 110.1, 115.1, 116.2, 118.0, 118.4, 119.9, 128.2, 128.8, 129.4, 130.1, 133.5, 133.8, 137.2, 137.4, 143.2, 143.9, 146.2, 162.6, 164.9. HPLC: 99%; t_R 8.70 min. EI-MS: m/z = 471 (M^+).

(*S*)-4′-((5-(3-(Methoxymethyl)-2,3-dihydrobenzo[*b*][1,4]-dioxin-6-yl)-1,3,4-oxadiazol-2-ylthio) methyl)biphenyl-2-carbonitrile (23c). Yield 84%, colorless solid. ^{1}H NMR (DMSO-d_6, 500 MHz): δ [ppm] = 3.33 (3H, s), 3.61 (2H, m), 4.10 (1H, m), 4.42 (2H, m), 4.66 (2H, s), 7.07 (1H, m), 7.44 (2H, m), 7.60 (6H, m), 7.78 (1H, td, J = 7.6 Hz, J = 1.3 Hz), 7.94 (1H, dd, J = 7.7 Hz, J = 0.9 Hz). ^{13}C NMR (DMSO-d_6, 125 MHz): δ [ppm] = 35.2, 58.7, 65.2, 70.1, 71.9, 110.1, 115.1, 116.2, 117.9, 118.4, 119.9, 128.2, 128.6, 129.4, 130.1, 133.5, 133.8, 137.2, 137.4, 143.2, 143.9, 146.2, 162.6, 164.9.

Table 5. Small Kinase Panel Values

kinase	enzyme conc (nM)	ATP conc (μM)	peptide used	peptide conc (μM)	buffer
GSK-3β	2	12.5	Ser/Thr 9 peptide	2	50 mM Hepes pH 7.5, 10 mM $MgCl_2$, 1 mM EGTA, 0.01% (w/v) Brij-35
GSK-3α	0.5	12.5	Ser/Thr 9 peptide	2	50 mM Hepes pH 7.5, 10 mM $MgCl_2$, 1 mM EGTA, 0.01% (w/v) Brij-35
CKIε	12	32	Ser/Thr 11 peptide	2	50 mM Hepes pH 7.5, 10 mM $MgCl_2$, 1 mM EGTA, 0.01% (w/v) Brij-35
Cdk5	10	12.5	Ser/Thr 12 peptide	2	50 mM Hepes pH 7.5, 10 mM $MgCl_2$, 1 mM EGTA, 0.01% (w/v) Brij-35
AurKA	20	10	Ser/Thr 1 peptide	2	50 mM Hepes pH 7.5, 10 mM $MgCl_2$, 1 mM EGTA, 0.01% (w/v) Brij-35
PKCα	0.15	10	Ser/Thr 7 peptide	2	50 mM Hepes pH 7.5, 10 mM $MgCl_2$, 1 mM EGTA, 0.01% (w/v) Brij-35

HPLC: 100%; t_R 8.65 min. EI-MS: m/z = 471 (M^+). HRMS (EI): m/z calcd for $C_{26}H_{21}N_3O_4S$ 471.1253, found 471.1269.

Compound **24b** was prepared in a similar manner to that described for **24a**.

(*R*)-4′-((5-(3-(Hydroxymethyl)-2,3-dihydrobenzo[*b*][1,4]-dioxin-6-yl)-1,3,4-oxadiazol-2-ylthio) methyl)biphenyl-2-carbonitrile (24b). Yield 79%, light-yellow solid. ^{1}H NMR (DMSO-d_6, 500 MHz): δ [ppm] = 3.40 (1H, s, br), 3.59 (2H, m), 4.04 (1H, m), 4.15 (1H, m), 4.34 (1H, dd, J = 11.5 Hz, J = 2.3 Hz), 4.57 (2H, s), 6.98 (1H, d, J = 8.3 Hz), 7.35 (2H, m), 7.53 (6H, m), 7.70 (1H, td, J = 7.7 Hz, J = 1.3 Hz), 7.85 (1H, dd, J = 7.7 Hz, J = 0.9 Hz). ^{13}C NMR (DMSO-d_6, 125 MHz): δ [ppm] = 35.4, 59.6, 65.4, 73.7, 110.1, 115.0, 116.1, 117.9, 118.5, 119.8, 128.2, 128.8, 129.3, 130.1, 133.4, 133.8, 137.1, 137.4, 143.5, 144.0, 146.2, 162.5, 164.9. HPLC: 95%; t_R 7.48 min. EI-MS: m/z = 457 (M^+).

(*S*)-((7-(5-(2′-Cyanobiphenyl-4-yl)methylthio)-1,3,4-oxadiazol-2-yl)-2,3-dihydrobenzo[*b*][1,4] dioxin-2-yl)-methylmethanesulfonate (25). To a solution of **24b** (238 mg, 0.52 mmol) in 10 mL of DCM was added Et_3N (0.72 mL, 5.2 mmol) followed by addition of methanesulfonyl chloride (402 μL, 5.2 mmol) at 0 °C. The reaction mixture was stirred at the same temperature for 1 h and further stirred at room temperature for 4 h. After treating with saturated $NaHCO_3$ solution, the reaction mixture was extracted with DCM. The combined organic layer was dried over $MgSO_4$, concentrated, and purified by column chromatography (EtOAc/cyclohexane, 1:1) to provide **25** (273 mg, 98%) yellow oil. ^{1}H NMR (DMSO-d_6, 500 MHz): δ [ppm] = 3.26 (3H, s), 4.17 (1H, m), 4.45 (1H, m), 4.50 (1H, dd, J = 11.6 Hz, J = 2.4 Hz), 4.55 (1H, dd, J = 11.6 Hz, J = 3.3 Hz), 4.62 (1H, m), 4.67 (2H, s), 7.11 (1H, d, J = 8.1 Hz), 7.48 (2H, m), 7.61 (6H, m), 7.77 (1H, td, J = 7.6 Hz, J = 1.3 Hz), 7.95 (1H, dd, J = 7.7 Hz, J = 0.8 Hz). ^{13}C NMR (DMSO-d_6, 125 MHz): δ [ppm] = 35.4, 36.8, 64.3, 67.8, 70.9, 110.1, 115.2, 116.4, 118.2, 118.5, 120.3, 128.2, 128.8, 129.4, 130.1, 133.5, 133.8, 137.1, 137.4, 142.7, 143.9, 145.9, 162.7, 164.9. HPLC: 96%; t_R 8.46 min. EI-MS: m/z = 535 (M^+).

(*R*)-4′-((5-(3-((2,2-Dimethoxyethylamino)methyl)-2,3-dihydrobenzo[*b*][1,4]dioxin-6-yl)-1,3,4-oxadiazol-2-ylthio)-methyl)biphenyl-2-carbonitrile (26). To a stirred solution of **25** (69 mg, 0.13 mmol) in 2 mL of THF was added 2,2-dimethoxyethylamine (140 μL, 1.3 mmol) and NEt_3 (180 μL, 1.3 mmol) at 0 °C, and the reaction mixture was stirred at room temperature for 5 days. The mixture was diluted with water and extracted with EtOAc. The organic layer was washed with brine and dried over $MgSO_4$. The solvent was evaporated under reduced pressure and the crude product purified by silica gel column chromatography (MeOH/EtOAc, 1:10) to give **26** (58 mg, 83%) as a dark-yellow oil. ^{1}H NMR (DMSO-d_6, 500 MHz): δ [ppm] = 1.91 (1H, m), 2.61 (2H, dd, J = 5.4 Hz, J = 0.7 Hz), 2.80 (2H, m), 3.18 (3H, s), 3.19 (3H, s), 4.00 (1H, m), 4.17 (1H, m), 4.30 (2H, m), 4.54 (2H, s), 6.87 (1H, m), 7.32 (2H, m), 7.44 (1H, dd, J = 7.6 Hz, J = 1.2 Hz), 7.46 (3H, m), 7.52 (2H, m), 7.64 (1H, td, J = 7.8 Hz, J = 1.3 Hz), 7.74 (1H, m). ^{13}C NMR (DMSO-d_6, 125 MHz): δ [ppm] = 36.7, 50.2, 52.1, 53.8, 53.9, 67.7, 74.1, 104.9, 111.8, 116.5, 117.8, 118.7, 119.1, 120.8, 129.0, 130.0, 130.4, 131.1, 134.1, 134.7, 138.4, 138.8, 144.7, 145.4, 147.6, 163.7, 166.3. HPLC: 95%; t_R 6.34 min. EI-MS: m/z = 544 (M^+).

GSK-3β in Vitro Assay. Purified GSK-3β (0.5 μg) was incubated in a reaction mixture of 50 mM Tris pH 7.3, 10 mM $MgAc_2$, 0.01% β-mercaptoethanol, ^{32}P[γ-ATP](100 μM, 0.5 μci/assay), and 100 μM of peptide substrate, pIRS-1 (RREGGMSRPAS(p)VDG (1). New molecules were added at various concentrations (1, 10, and 100 μM), and the reaction mixture was incubated for 15 min at 30 °C. The reactions were stopped, spotted on p81 paper (Whatman), washed with 10 mM phosphoric acid, and counted for radioactivity.[50] GSK-3β activity was calculated as the percentage of GSK-3β activity in the absence of inhibitor that was designated to 100%.

Small Kinase Panel. Compounds were serially diluted 1/3 in neat DMSO (10 serial dilutions), and these dilutions were further diluted 1/25 with reaction buffer. Then 2.5 μL of these solutions were added to the reaction mixture described below so that final compound concentration in the assay ranges from 100 μM to 5 nM in 1% (v/v) DMSO. When compounds showed high inhibition at 5 nM and therefore the data could not be fitted to the corresponding equation, they were re-evaluated in a new range from 400 nM to 20 pM (Table 5).

The enzymatic activity of the kinases was determined with a commercial system based on the Z′-LYTE technology, available from Invitrogen Life Technologies (Carlsbad, CA, USA), using human recombinant kinases as the enzyme source. This technology utilizes the fluorescence resonance energy transfer ("FRET") process between fluorescein and coumarin. The assay principle is based on the differential sensitivity of phosphorylated and nonphosphorylated peptide to proteolytic cleavage, which precludes the energy transfer process between the two fluorophores attached to both sides of the cleavage site. Hence, enzymatic phosphorylation will yield a phosphopeptide, which cannot be hydrolyzed by a suitable protease and energy transfer between the two fluorophores will occur. Opposingly, lack of phosphorylation will cause peptide hydrolysis hence lack of energy transfer as. The assay was performed in 96-well black plates, in a final volume of 10 μL, with components as detailed in Tables 1, 3, and 4.

In Vivo Activity on Zebrafish Embryos. The wt zebrafish was used in this study. The embryos were collected and placed into 24-well plates, 10 embryos per well, and maintained in E2 medium at ∼28 °C. Compounds were added 5 hpf (50% epiboly) and the embryos allowed to grow in chemical compound solution up to 2 days. The phenotypes were compared using the Axio Scope.A1 microscope system from Carl Zeiss at 44−48 hpf.[36,37,51]

Animal Husbandry. All animal experiment were conducted and documented according to the federal and local regulation. All embryo testing was stopped at day 5 of embryonic development.

SH-SY5Y Neuroblastoma Cells. SH-SY5Y neuroblastoma cells stably transfected with Tau.P301L in the pcDNA3 vector were grown to confluency in 6-well cluster plates (∼800000 cells/well) in DMEM-F12 medium supplemented with Glutamax and 15% fetal calf serum. The medium contained gentamycin (50 μg/mL) as general antibiotic and Geneticin (250 μg/mL) to maintain selection pressure on transfected cells. Cells were grown at 37 °C in a humidified incubator in an atmosphere of 5.0% CO_2 in air. Stock solutions of the

compounds in DMSO were added to serum-free culture medium to the specified concentrations, using DMSO in the same final concentrations as control. Cells were incubated with the compounds at 37 °C for the indicated periods of time. After incubation, spent medium was removed and cells washed once with PBS containing Ca^{2+} and Mg^{2+}. The cells were rapidly harvested by mechanical scraping after addition of hot 62.5 mM Tris pH 6.8 buffer, containing 1% SDS (180 μL per well). Protein extracts were collected by aspiration and reduced and denatured by addition of 1% β-mercaptoethanol and boiling for 10 min. After separation by SDS-PAGE on 10% Tris-glycine SDS-PAGE, proteins were analyzed by Western blotting using the ECL-system.[52] In brief, after SDS-PAGE, the separated proteins were transferred to nitrocellulose filter-sheets, which were treated against nonspecific binding by incubation in 5% nonfat milk in Tris buffered saline (TBS: 10 mM Tris.HCl, pH 7.2, 0.9% sodium chloride, 0.1% Tween). Blots were subsequently incubated with primary antibodies specifically directed against total protein tau or against its selected phosphorylated epitopes, as specified in Results and Discussion and in the figure legends. After incubation with suitably labeled secondary antibodies, the resulting immune reactions were recorded and analyzed digitally with dedicated apparatus and software (LAS4000, Image-QuantTL, GE Healthcare, Brussels, Belgium). Data for tau and phospho-tau were normalized against actin, revealed by Western blotting of the same samples on the same blots.

Docking Simulations. Molecular docking of **15a** into the X-ray structure of GSK-3β (PDB code: 3F88) was carried out using the Glide 5.5 program.[53] Maestro 9.0.211 was employed as the graphical user interface, and Figure 2 was rendered by the Chimera software package.[54,55]

Ligand and Protein Setup. The inhibitor structure was first generated through the Dundee PRODRG2 server.[56] Then geometry optimized ligand was prepared using Lig-Prep 2.3 as implemented in Maestro. The target protein was prepared through the Protein Preparation Wizard of the graphical user interface Maestro and the OPLS-2001 force field. Water molecules were removed. Hydrogen atoms were added, and minimization was performed until the rmsd of all heavy atoms was within 0.3 Å of the crystallographically determined positions. The binding pocket was identified by placing a 20 Å cube centered on the mass center of the cocrystallized inhibitor. Molecular docking calculations were performed with the aid of Glide 5.5 in extra-precision (XP) mode, using Glidescore for ligand ranking.[57,58] For multiple ligand docking experiments, an output maximum of 5000 ligand poses per docking run with a limit of 100 poses for each ligand was adopted.

Homology Modeling. The homology model was built using the crystal structure of GSK-3β (PDB code: 3F88). The sequence identity between GSK-3α and GSK-3β is 61%. The alignment was performed by Prime, which calculates alignments using a combination of sequence and secondary structure information. The sequence of the human GSK-3α was obtained from the Universal Protein Resource (http://www.uniprot.org/) (code: P49840) and aligned using Prime. The homology model was inspected to ensure that the side chains of the conserved residues were aligned to the template.

■ ASSOCIATED CONTENT

Supporting Information

Homology modeling, in vitro pharmacology, bioavailability profile of compound **14d** and NMR data of compounds **5b**, **5c**, **6b**, **6c**, **14b**, **14c**, **14d**, **15a**, **15b**, **16a**, **23a**, **23b**, and **23c**. This material is available free of charge via the Internet at http://pubs.acs.org.

■ AUTHOR INFORMATION

Corresponding Author

*Phone: +496151-164531. Fax: +496151-163278. E-mail: schmidt_boris@t-online.de (B.S.); Fabio.Lo-Monte@gmx.de (F.L.).

Notes

The authors declare no competing financial interest.

■ ACKNOWLEDGMENTS

This work was supported by a collaborative project financed by the 7th Framework Program of the European Union (neuro.GSK3).

■ ABBREVIATIONS USED

ATP, adenosine triphosphate; AD, Alzheimer's disease; BBB, blood−brain barrier; Cdk, cyclin-dependent kinase; GSK-3, glycogen synthase kinase-3; DMF, dimethylformamide; DMSO, dimethyl sulfoxide; EtOAc, ethyl acetate; EtOH, ethanol; hpf, hours post fertilization; HPLC, high performance liquid chromatography; MeOH, methanol; SAR, structure−activity relationship

■ REFERENCES

(1) Engel, T.; Goni-Oliver, P.; Gómez de Barreda, E.; Lucas, J. J; Hernandez, F.; Avila, J. Lithium, a Potential Protective Drug in Alzheimer's Disease. *Neurodegenerative Dis.* **2008**, *5*, 247−249.

(2) Citron, M. Alzheimer's disease: strategies for disease modification. *Nature Rev. Drug Discovery* **2010**, *9*, 387−397.

(3) Mazanetz, M. P.; Fischer, P. M. Untangling tau hyperphosphorylation in drug design for neurodegenerative diseases. *Nature Rev. Drug Discovery* **2007**, *6*, 464−479.

(4) Cohen, P.; Goedert, M. GSK3 Inhibitors: Development and Therapeutic Potential. *Nature Rev. Drug Discovery* **2004**, *3*, 479−487.

(5) Saitoh, M.; Kunitomo, J.; Kimura, E.; Iwashita, H.; Uno, Y.; Onishi, T.; Uchiyama, N.; Kawamoto, T.; Tanaka, T.; Mol, C. D.; Dougan, D. R.; Textor, G. P.; Snell, G. P.; Takizawa, M.; Itoh, F.; Kori, M. 2-[3-[4-(Alkylsulfinyl)phenyl]-1-benzofuran-5-yl]-5-methyl-1,3,4-oxadiazole Derivatives as Novel Inhibitors of Glycogen Synthase Kinase-3β with Good Brain Permeability. *J. Med. Chem.* **2009**, *52*, 6270−6286.

(6) Martinez, A. Preclinical Efficacy on GSK-3 Inhibitors: Towards a Future Generation of Powerful Drugs. *Med. Res. Rev.* **2008**, *28*, 773−796.

(7) Frame, S.; Cohen, P. GSK3 takes centre stage more than 20 years after its discovery. *Biochem. J.* **2001**, *359*, 1−16.

(8) Cohen, P.; Frame, S. The renaissance of GSK3. *Nature Rev. Mol. Cell Biol.* **2001**, *2*, 769−775.

(9) Martinez, A.; Castro, A.; Dorronsoro, I.; Alonso, M. Glycogen Synthase Kinase 3 (GSK-3)—Inhibitors as New Promising Drugs for Diabetes, Neurodegeneration, Cancer and Inflammation. *Med. Res. Rev.* **2002**, *22*, 373−384.

(10) Bhat, R. V.; Budd Haeberlein, S. L.; Avila, J. Glycogen synthase kinase 3: a drug target for CNS therapies. *J. Neurochem.* **2004**, *89*, 1313−1317.

(11) Zou, H.; Zhou, L.; Li, Y.; Cui, Y.; Zhong, H.; Pan, Z.; Yan, Z.; Quan, J. Benzo[*e*]isoindole-1,3-diones as potential Inhibitors of Glycogen Synthase Kinase-3 (GSK-3). Synthesis, Kinase Inhibitory Activity, Zebrafish Phenotype, and Modeling of Binding Mode. *J. Med. Chem.* **2010**, *53*, 994−1003.

(12) Kaidanovich-Beilin, O.; Lipina, T. V.; Takao, K.; van Eede, M.; Hattori, S.; Laliberté, C.; Khan, M.; Pkamoto, K.; Chambers, J. W.; Fletcher, P. J.; MacAulay, K.; Doble, B. W.; Henkelman, M.; Miyakawa, T.; Roder, J.; Woodgett, J. R. Abnormalities in brain structure and behavior in GSK-3alpha mutant mice. *Mol. Brain* **2009**, *2*, 1−23.

(13) Alon, L. T.; Pietrokovski, S.; Barkan, S.; Avrahami, L.; Kaidanovich-Beilin, O.; Woodgett, J. R.; Barnea, A.; Eldar-Finkelman, H. Selective loss of glycogen synthase kinase-3α in birds reveals distinct roles for GSK-3 isozymes in tau phosphorylation. *FEBS Lett.* **2011**, *585*, 1158−1162.

(14) Phiel, C. J.; Wislon, C. A.; Lee, V. M.-Y.; Klein, P. S. GSK-3α regulates production of Alzheimer's disease amyloid-β peptides. *Nature* **2003**, *423*, 435−439.
(15) Zhou, J.; Lal, H.; Chen, X.; Shang, X.; Song, J.; Li, Y.; Kerkela, R.; Doble, B. W.; MacAulay, K.; DeCaul, M.; Koch, W. J.; Farber, J.; Woodgett, J.; Gao, E.; Force, T. GSK-3α directly regulates β-adrenergic signaling and the response of the heart to hemodynamic stress in mice. *J. Clin. Invest.* **2010**, *120*, 2280−2291.
(16) Banerji, V.; Frumm, S. M.; Ross, K. N.; Li, L. S.; Schinzel, A. C.; Hahn, C. K.; Kakoza, R. M.; Chow, K. T.; Ross, L.; Alexe, G.; Tolliday, N.; Inguilizian, H.; Galinsky, I.; Stone, R. M.; DeAngelo, D. J.; Roti, G.; Aster, J. C.; Hahn, W. C.; Kung, A. L.; Stegmaier, K. The intersection of genetic and chemical genomic screens identifies GSK-3α as a target in human acute myeloid leukemia. *J. Clin. Invest.* **2012**, *122*, 935−947.
(17) Dajani, R.; Fraser, E.; Roe, S. M.; Young, N.; Good, V.; Dale, T. C.; Pearl, L. H. Crystal Structure of Glycogen Synthase Kinase 3β: Structural Basis for Phosphate-Primed Substrate Specificity and Autoinhibition. *Cell* **2001**, *105*, 721−732.
(18) Leclerc, S.; Garnier, M.; Hoessel, R.; Marko, D.; Bibb, J. A.; Snyder, G. L.; Greengard, P.; Biernat, J.; Wu, Y. Z.; Mandelkow, E. M.; Eisenbrand, G.; Meijer, L. Indirubins inhibit glycogen synthase kinase-3 beta and CDK5/p25, two protein kinases involved in abnormal tau phosphorylation in Alzheimer's disease. A property common to most cyclin-dependent kinase inhibitors? *J. Biol. Chem.* **2001**, *276*, 251−260.
(19) Leost, M.; Schultz, C.; Link, A.; Wu, Y. Z.; Biernat, J.; Mandelkow, E. M.; Bibb, J. A.; Snyder, G. L.; Greengard, P.; Zaharevitz, D. W.; Gussio, R.; Senderowicz, A. M.; Sausville, E. A.; Kunick, C.; Meijer, L. Paullones are potent inhibitors of glycogen synthase kinase-3beta and cyclin-dependent kinase 5/p25. *Eur. J. Biochem.* **2000**, *267*, 5983−5994.
(20) Martinez, A.; Alonso, M.; Castro, A.; Perez, C.; Moreno, F. J. First non-ATP competitive glycogen synthase kinase 3 beta (GSK-3beta) inhibitors: thiadiazolidinones (TDZD) as potential drugs for the treatment of Alzheimer's disease. *J. Med. Chem.* **2002**, *45*, 1292−1299.
(21) Smith, D. G.; Buffet, M.; Fenwick, A. E.; Haigh, D.; Ife, R. J.; Saunders, M.; Slingsby, B. P.; Stacey, R.; Ward, R. W. 3-Anilino-4-arylmaleimides: potent and selective inhibitors of glycogen synthase kinase-3 (GSK-3). *Bioorg. Med. Chem. Lett.* **2001**, *11*, 635−639.
(22) Lo Monte, F.; Kramer, T.; Boländer, A.; Plotkin, B.; Eldar-Finkelman, H.; Fuertes, A.; Dominguez, J. M.; Schmidt, B. Synthesis and biological evaluation of glycogen synthase kinase 3 (GSK-3) inhibitors: a fast and atom efficient access to 1-aryl-3-benzylureas. *Bioorg. Med. Chem. Lett.* **2011**, *21*, 5610−5615.
(23) Eldar-Finkelman, H.; Martinez, A. GSK-3 inhibitors: preclinical and clinical focus on CNS. *Front. Mol. Neurosci.* **2011**, *4*, 1−18.
(24) Kramer, T.; Schmidt, B.; Lo Monte, F. Small-molecule inhibitors of GSK-3—Structural insights and their application to Alzheimer's disease models. *Int. J. Alzheimer's Dis.* **2012**, in press.
(25) Naerum, L.; Norskov-Lauritsen, L.; Olesen, P. H. Scaffold hopping and optimization towards libraries of glycogen synthase kinase-3 inhibitors. *Bioorg. Med. Chem. Lett.* **2002**, *12*, 1525−1528.
(26) Saitoh, M.; Kunitomo, J.; Kimura, E.; Hayase, Y.; Kobayashi, H.; Uchiyama, N.; Kawamoto, T.; Tanaka, T.; Mol, C. D.; Dougan, D. R.; Textor, G. S.; Snell, G. P.; Itoh, F. Design, synthesis and structure−activity relationships of 1,3,4-oxadiazole derivatives as novel inhibitors of glycogen synthase kinase-3beta. *Bioorg. Med. Chem.* **2009**, *17*, 2017−2029.
(27) Oertby, E.; Pictet, A. Derivatives of Piperonylic Acid. *Ber. Dtsch. Chem. Ges.* **1910**, *43*, 1336−1340.
(28) Yu, T.; Hsu, L.; Wu, S. *Huaxue Xuebao* **1958**, *24*, 170−173.
(29) Mc Fayden, J. S.; Stevens, T. S. New method for the conversion of acids into aldehydes. *J. Chem. Soc.* **1936**, 584−587.
(30) Konig, H. B.; Seifken, W.; Offe, H. A. Sulfur-containing derivatives of pyridine carboxylic acids and compounds derived therefrom. *Chem. Ber.* **1954**, *87*, 825−834.
(31) Mazzone, G.; Bonina, F.; Arrigo-Reina, R. Synthesis and pharmacological activities of some 2-(alkylaminoalkyl)mercapto-5-aryl-(1,3,4-oxadiazoles). *Farmaco, Ed. Sci.* **1977**, *32*, 414−429.
(32) Omar, R. H.; El-Fattah, B. A. Synthesis of certain pyridyl 1,3,4-oxadiazoles of biological interest and study of the cleavage of certain substituted oxadiazole rings with primary amines. *Egypt. J. Pharm. Sci.* **1985**, *24*, 49−56.
(33) Akwabi-Ameyaw, A.; Bass, J. Y.; Caldwell, R. D.; Caravella, J. A.; Chen, L.; Creech, K. L.; Deaton, D. N.; Madauss, K. P.; Marr, H. B.; McFadyen, R. B.; Miller, A. B.; Navas, F., III; Parks, D. J.; Spearing, P. K.; Todd, D.; Williams, S. P.; Wisely, G. B. FXR agonist activity of conformationally constrained analogs of GW 4064. *Bioorg. Med. Chem.* **2009**, *19*, 4733−4739.
(34) Dolezal, M.; Palek, L.; Vinsova, J.; Buchta, V.; Jampilek, J.; Kralova, K. Substituted Pyrazinecarboxamides: Synthesis and Biological Evaluation. *Molecules* **2006**, *11*, 242−256.
(35) Schmidt, B.; Meid, D.; Kieser, D. Safe and fast tetrazole formation in ionic liquids. *Tetrahedron* **2007**, *63*, 492−496.
(36) Funke, A.; Paulsen, A.; Cibrario, N. Chloromethyl- and aminomethyl(acetyl)benzodioxan isomers and derivatives resulting from oxidation of the acetyl group. *Bull. Soc. Chim. Fr.* **1958**, 470−473.
(37) Hormann, R. E.; Tice, C. M.; Chortyk, O.; Smith, H.; Meteyer, T. Diacylhydrazine ligands for modulating the expression of exogenous genes in mammalian systems via an ecdysone receptor complex. PCT-WO 2004/072254 2004, pp 1−120.
(38) Alksnis, A. F.; Surna, J. A. Preparation of Benzodioxane Derivatives. GB Patent 1109275 1965, pp 1−2.
(39) Satoh, Y.; Powers, C.; Toledo, L. M.; Kowalski, T. J.; Peters, P. A.; Kimble, E. F. Derivatives of 2-[[*N*-(Aminocarbonyl)-*N*-hydroxyamino]methyl]-1,4-benzodioxan as Orally Active 5-Lipoxygenase Inhibitors. *J. Med. Chem.* **1995**, *38*, 68−75.
(40) Lee, J. Y.; Park, Y. K.; Seo, S. H.; Yang, B.; Park, H.; Lee, Y. S. 7-Substituted-[1,4]dioxano[2,3-*g*]quinazolines as Inhibitors of Epidermal Growth Factor Receptor Kinase. *Arch. Pharm. Pharm. Med. Chem.* **2002**, *10*, 487−494.
(41) Feng, L.; Geisselbrecht, Y.; Black, S.; Wilbuer, A.; Atilla-Gokcumen, G. E.; Filippakopoulos, P.; Kräling, K.; Celik, M. A.; Harms, K.; Maksimoska, J.; Marmorstein, R.; Frenking, G.; Knapp, S.; Essen, L.; Meggers, E. Structurally Sophisticated Octahedral Metal Complexes as Highly Selective Protein Kinase Inhibitors. *J. Am. Chem. Soc.* **2011**, *133*, 5976−5986.
(42) Limongelli, V.; Marinelli, L.; Cosconati, S.; La Motta, C.; Sartini, S.; Mugnaini, L.; Da Settimo, F.; Novellino, E.; Parrinello, M. Sampling protein motion and solvent effect during ligand binding. *Proc. Natl. Acad. Sci. U.S.A.* **2012**, *109*, 1467−1472.
(43) Limongelli, V.; Bonomi, M.; Marinelli, L.; Gervasio, F. L.; Cavalli, A.; Novellino, E.; Parrinello, M. Molecular basis of cyclooxygenase enzymes (COXs) selective inhibition. *Proc. Natl. Acad. Sci. U.S.A.* **2010**, *107*, 5411−5416.
(44) Atilla-Gokcumen, G. E.; Williams, D. S.; Bregman, H.; Pagano, N.; Meggers, E. Organometallic Compounds with Biological Activity: A Very Selective and Highly Potent Cellular Inhibitor for Glycogen Synthase Kinase 3. *ChemBioChem* **2006**, *7*, 1443−1450.
(45) Paquet, D.; Bhat, R.; Sydow, A.; Mandelkow, E.; Berg, S.; Hellberg, S.; Fälting, J.; Distel, M.; Köster, R. W.; Schmid, B.; Haass, C. A zebrafish model of tauopathy allows in vivo imaging of neuronal cell death and drug evaluation. *J. Clin. Invest.* **2009**, *119*, 1382−1395.
(46) Azoulay-Alfaguter, I.; Yaffe, Y.; Licht-Murava, A.; Urbanska, M.; Jaworski, J.; Pietrokovski, S.; Hirschberg, K.; Eldar-Finkelman, H. Distinct molecular regulation of glycogen synthase kinase-3alpha isozyme controlled by its N-terminal region: functional role in calcium/calpain signaling. *J. Biol. Chem.* **2011**, *286*, 13470−13480.
(47) Jaworski, T.; Dewachter, I.; Lechat, B.; Gees, M.; Kremer, A.; Demedts, D.; Borghgreaf, P.; Devijver, H.; Kügler, S.; Patel, S.; Woodgett, J. R.; Van Leuven, F. GSK-3α/β kinases and amyloid production in vivo. *Nature* **2011**, *480*, E4−E5.
(48) Phiel, C. J.; Wislon, C. A.; Lee, V. M.-Y.; Klein, P. S. Phiel et al. reply. *Nature* **2011**, *480*, E6.

(49) Tromp, R. A.; van Ameijde, S.; Pütz, C.; Sundermann, C.; Sundermann, B; von Frijtag Drabbe Künzel, J. K.; IJzerman, P. Inhibition of Nucleoside Transport by New Analogues of 4-Nitrobenzylthioinosine: Replacement of the Ribose Moiety by Substituted Benzyl Groups. *J. Med. Chem.* **2004**, *47*, 5441−5450.
(50) Liberman, Z.; Eldar-Finkelman, H. Serine 332 phosphorylation of insulin receptor substrate-1 by glycogen synthase kinase-3 attenuates insulin signaling. *J. Biol. Chem.* **2005**, *280*, 4422−4428.
(51) Kimmel, C. B.; Ballard, W. W.; Kimmel, S. R.; Ullmann, B.; Schilling, T. F. Stages of Embryonic Development of the Zebrafish. *Dev. Dyn.* **1995**, *203*, 253−310.
(52) Dutschmann, M.; Menuet, C.; Stettner, G. M.; Gertreau, C.; Borghgraef, P.; Devijver, H.; Gielis, L.; Hilaire, G.; Van Leuven, F. Upper airway dysfunction of Tau.P301L mice correlates with tauopathy in midbrain and ponto-medullary brainstem nuclei. *J. Neurosci.* **2010**, *30*, 1810−1821.
(53) *Glide*, version 5.5; Schrödinger, LLC: New York, 2009.
(54) *Maestro*, version 9.0.211; Schrödinger, LLC: New York, 2009.
(55) Pettersen, E. F.; Goddard, T. D.; Huang, C. C.; Couch, G. S.; Greenblatt, D. M.; Meng, E. C.; Ferrin, T. E. UCSF chimera—a visualization system for exploratory research and analysis. *J. Comput. Chem.* **2004**, *25*, 1605−1612.
(56) Schuttelkopf, A. W.; van Aalten, D. M. PRODRG: a tool for high-throughput crystallography of protein−ligand complexes. *Acta Crystallogr., Sect. D: Biol. Crystallogr.* **2004**, *60*, 1355−1363.
(57) Friesner, R. A.; Murphy, R. B.; Repasky, M. P.; Frye, L. L.; Greenwood, J. R.; Halgren, T. A.; Sanschagrin, P. C.; Mainz, D. T. Extra precision glide: docking and scoring incorporating a model of hydrophobic enclosure for protein-ligand complexes. *J. Med. Chem.* **2006**, *49*, 6177−6196.
(58) Friesner, R. A.; Banks, J. L.; Murphy, R. B.; Halgren, T. A.; Klicic, J. J.; Mainz, D. T.; Repasky, M. P.; Knoll, E. H.; Shelley, M.; Perry, J. K.; Shaw, D. E.; Francis, P.; Shenkin, P. S. Glide: a new approach for rapid, accurate docking and scoring. 1. Method and assesment of docking accuracy. *J. Med. Chem.* **2004**, *47*, 1739−1749.